## REMARKS

Claims 1-8 and 16-19 were previously pending in this application. By this amendment, Applicant is canceling claims 6 and 17-19 without prejudice or disclaimer. Claims 1 and 8 have been amended. Claim 1 has been amended to remove a number of the meanings for $R_s/R_t$. In particular, $R_t$ has been limited to hydrogen and substituents of the alkyl/alkenyl type. $R_s$ has been limited such that it does not include hydrogen, substituents of the alkyl/alkenyl type, substituted heterocyclylalkyl, and unsubstituted aryl. In addition, the claim does not include the case where $R_s$ and $R_t$ form, together with nitrogen to which they are attached, a heterocyclic ring.

New claim 20 has been added, in which the meaning of the expressions "heterocyclic" and "substituted" is more explicitly defined.

As a result, claims 1-5, 7-8, 16 and 20 are pending for examination with claim 1 being the independent claim. No new matter has been added.

### Rejection Under 35 U.S.C. § 112, First Paragraph

The Examiner rejected claims 6-8 and 16-19 under 35 U.S.C. §112, first paragraph. With respect to the issue of claims breadth, reconsideration is respectfully requested in view of the substantial limitations inserted in the claims. These include important structural limitations to formula (I), as well as a substantial limitation in the number and type of diseases to be treated.

In particular, the objectionable reference to "diseases associated with overactivity of osteoclasts" has been deleted; the treatment of viral diseases, angiogenic diseases, AIDS, has further been deleted; and methods of prevention have been deleted as well.

The claimed method of treatment is now focused on osteoporosis and related osteopenic diseases, in view of the bone resorption activity discussed in the specification. The claims also include the treatment of tumours.

Responsive to the Examiner's request for experimental evidence, Applicant submits the results of pharmacological testing (Annex 1) whereby the compound of example 6 is reported to have both activities underlying the present claims, namely the V-ATPase inhibitory activity in the osteoclast, and a remarkable antitumour activity on liver, colon, and drug-resistant colon cell lines.

Further, current literature is hereby annexed (Annex 2), showing the effectiveness of V-ATPase inhibitors (in particular bafilomycin and concanamycin) to inhibit the growth of cells

resistant to classic antitumour agents such as anthracyclins and taxol derivatives. In particular, cf. the following passages:

Izumi et al., Cancer Treatment Reviews (2003) 29:541-549

*(p. 545): "Recently described specific inhibitors of mammalian V-ATPase belonging to the benzolactone enamide class, such as salicylihalamide, lobatamides and oximidines appear promising as anticancer agents. Among these agents, salicylihalamide A can discriminate between mammalian and non-mammalian V-ATPases."*

Torigoe et al., J. Biol. Chem. (2002) 277(39): 36534-36543

*(abstract) "...combination of the vacuolar $H^+$-ATPase (V-ATPase) inhibitor, bafilomycin A1, with TAS-103 enhanced apoptosis of KB [cancer] cells with an associated increase in caspase-3 activity. Our data suggest that the induction of V-ATPase expression is an anti-apoptotic defense, and V-ATPase inhibitors in combination with low-dose anticancer agents may provide a new therapeutic approach."*

Ouar et al., Biochem. J. (2003) 370, 185-193

*(abstract) "[the V-ATPase inhibitors concanamycin A] CCM A and bafilomycin A1 almost completely restored the sensitivity of these drug-resistant cells to daunomycin, doxorubicin and epirubicin. These findings indicate that lysosomotropic agents that impair the acidic-pH-dependent accumulation of weak-base chemotherapeutic drugs may reverse anthracycline resistance in MDR cells...."*

Given the knowledge in the art, as demonstrated above, and the teaching of the application, one of ordinary skill in the art would be enabled to practice the invention as now claimed without undue experimentation.

In view of the foregoing, Applicant respectfully requests withdrawal of the rejections made under 35 U.S.C. § 112, first paragraph.

Rejection Under 35 U.S.C. § 112, Second Paragraph

The Examiner maintained the rejection of claims 1, 8 and 23 (and probably claim 6) under 35 U.S.C. §112, second paragraph.

784629.1

With respect to the definitions considered unclear by the Examiner, Applicant notes the following:

Regarding "heterocyclyl": The specification gives a clear definition of this term: cf. page 5, lines 6-12, where the array of heteroatoms, the size of the rings and the nature of atoms as ring members is precisely explained. Accordingly the term "heterocyclyl" in the claims is not an appropriate basis for the rejection of the claims.

Regarding "substituted": In the specification there is a clear definition for this term, wherein the nature and number of substituents is specified: substituents for alkyl and alkenyl groups are defined on page 4, lines 13-14, and the paragraph bridging pages 4-5. Accordingly, the term "substituted" is not an appropriate basis for the rejection of the claims.

In any case, for mere sake of completeness Applicant has added a new claim 20, wherein the above originally disclosed definitions have been entered in the text of the claims.

To the extent that claim 6 was rejected, the rejection is moot in view of the cancellation of this claim.

In view of the foregoing, Applicant respectfully requests withdrawal of the rejections made under 35 U.S.C. § 112, second paragraph.


Rejection Under 35 U.S.C. § 102

The Examiner maintained the rejections of claims 1-3 and 5 under 35 U.S.C. § 102(a) as anticipated by Downing et al. (WO 95/30659), by Barraclough et al. (Eur. J. Med. Chem., 1992), and by King et al. (J. Chem. Soc. Perkin Trans., 1988). Claims 1-3 were rejected by compounds having Beilstein RN 5988985, 6009580, 208984 and 282385. Applicant respectfully traverses the rejections.

Claim 1 as amended does not overlap with the compounds disclosed in the cited references. In particular:

-       claim 1 does not include the case where both $R_s$ and $R_t$ are hydrogen. For this reason it is novel over compounds 4 and 15 of Barraclough, compound 22 of King, and RN 208984 of Beilstein;

-       claim 1 is novel over Beilstein's RN 282385, because it does not include the case where $R_s$ or $R_t$ is unsubstituted aryl; novelty is present also over RN 5988985 and

         6009580, because claim 1 does not include the case where $R_s$ and $R_t$ taken together form a heterocyclic group; and

-       no overlap exists with Downing because claim 1 does not include the case where $R_s$ and $R_t$ is a substituted heterocyclyl-alkyl.

Accordingly, all novelty objections have been overcome and Applicant respectfully requests withdrawal of the rejections made under 35 U.S.C. § 102.

## Rejection Under 35 U.S.C. § 103

The Examiner maintained rejected claims 1-3 and 5 under 35 U.S.C. § 103 as unpatentable over Downing et al. (WO 95/30659). Applicant respectfully traverses the rejection and requests reconsideration in view of the amendment made to claim 1.

The Examiner considers it obvious for one of ordinary skill in the art to select compounds similar to those of the cited prior art, with the expectation that their property would remain the same; in the second Office Action, maintenance of this objection was based on the reasons raised in the 102 rejection.

Given that the anticipation rejection is now moot in view of the amendment to claim 1, and given that the compounds of the prior art are no longer species within the genus claimed, the 103 rejection is no longer applicable.

In addition, Applicant submits that the properties of the compounds claimed are certainly not the same as in the cited prior art. In fact the properties are completely different and unrelated: Barraclough teaches inotropic agents, i.e., cardiostimulants; King shows synthetic products, with no biological activity; Beilstein shows only chemical structures, with no biological activities; and Downing teaches antipsychotic agents against schizophrenia and related psychoses.

Quite differently, the claimed compounds have activity against osteoporosis and tumours, i.e., activities new and completely unrelated to those of the prior art reviewed above: it is absolutely unobvious that compounds merely used in synthetic studies or used as a cardiostimulant, an antipsychotic and any derivatives thereof could have utility against osteoporosis and tumours.

Accordingly, a skilled person in the art would not have been motivated, starting from the above-mentioned prior art, the present new compounds useful against osteoporosis and tumours.

784629.1

Therefore, in view of the present claim amendments and reasons in support of the amended claims, the present claims are not obvious over the Downing reference.

Accordingly, Applicant respectfully requests withdrawal of the rejections made under 35 U.S.C. § 103.

## CONCLUSION

In view of the foregoing amendments and remarks, this application should now be in condition for allowance. A notice to this effect is respectfully requested. If the Examiner believes, after this response, that the application is not in condition for allowance, the Examiner is requested to call the Applicant's attorney at the telephone number listed below.

If this response is not considered timely filed and if a request for an extension of time is otherwise absent, Applicant hereby requests any necessary extension of time. If there is a fee occasioned by this response, including an extension fee, that is not covered by an enclosed check, please charge any deficiency to Deposit Account No. 23/2825.

Respectfully submitted,
*Farina, et al., Applicant*

John R. Van Amsterdam, Reg. No. 40,212
Wolf, Greenfield & Sacks, P.C.
600 Atlantic Avenue
Boston, Massachusetts 02210-2211
Telephone: (617) 646-8000

Docket No.: N0424.70005US00
Date: April 14, 2004
**x04/14/04**

784629.1

## 1.     V-ATPase INHIBITORY ACTIVITY

V-ATPase inhibitory activity for the compound of Example 6:  $IC_{50}$ in osteoclasts = 8nM.

## 2.     ANTITUMOR ACTIVITY

The compound of example 6 was tested for its ability to inhibit the growth of tumour cells in vitro:

| Tumour cell line | $GI_{50}$ (microM) |
|---|---|
| Colon HT29 | 0.56 |
| Colon HT29 resistant | 0.27 |
| Liver HepG2 | 0.71 |

**ANNEX 1**

## 1. V-APTase INHIBITORY ACTIVITY

V-ATPase inhibitory activity for the compound of example 6: $IC_{50}$ in osteoclast = 8 nM.

## 2. ANTITUMOR ACTIVITY

The compound of example 6 was tested for its ability to inhibit the growth of tumour cells in vitro:

| Tumour cell line | $GI_{50}$ (microM) |
|---|---|
| Colon HT29 | 0.56 |
| Colon HT29 resistant | 0.27 |
| Liver HepG2 | 0.71 |

**LABORATORY–CLINIC INTERFACE**

CANCER
TREATMENT
REVIEWS

# Cellular pH regulators: potentially promising molecular targets for cancer chemotherapy

**Hiroto Izumi, Takayuki Torigoe, Hiroshi Ishiguchi, Hidetaka Uramoto, Yoichiro Yoshida, Mizuho Tanabe, Tomoko Ise, Tadashi Murakami, Takeshi Yoshida, Minoru Nomoto and Kimitoshi Kohno**

*Department of Molecular Biology, University of Occupational and Environmental Health, School of medicine, Fukuoka 807-8555, Japan*

One of the major obstacles to the successful treatment of cancer is the complex biology of solid tumour development. Although regulation of intracellular pH has been shown to be critically important for many cellular functions, pH regulation has not been fully investigated in the field of cancer. It has, however, been shown that cellular pH is crucial for biological functions such as cell proliferation, invasion and metastasis, drug resistance and apoptosis. Hypoxic conditions are often observed during the development of solid tumours and lead to intracellular and extracellular acidosis. Cellular acidosis has been shown to be a trigger in the early phase of apoptosis and leads to activation of endonucleases inducing DNA fragmentation. To avoid intracellular acidification under such conditions, pH regulators are thought to be up-regulated in tumour cells. Four major types of pH regulator have been identified: the proton pump, the sodium–proton exchanger family (NHE), the bicarbonate transporter family (BCT) and the monocarboxylate transporter family (MCT). Here, we describe the structure and function of pH regulators expressed in tumour tissue. Understanding pH regulation in tumour cells may provide new ways of inducing tumour-specific apoptosis, thus aiding cancer chemotherapy.
© 2003 Elsevier Ltd. All rights reserved.

**Key words:** Cancer chemotherapy; proton pump; V-ATPase; sodium–proton exchanger; bicarbonate transporter; monocarboxylate transporter; hypoxia; apoptosis.

## SOLID TUMOUR GROWTH AND PH

In order to overcome cancer, it is important that we gain an understanding of the molecular mechanisms involved in the growth of solid tumours. In general, tumour cells up-regulate glycolysis and grow in a hypoxic microenvironment. Highly proliferative cancer cells produce a large amount of metabolic acid generated by glycolysis, glucose utilization and lactic acid production and increase proton efflux, thus preventing apoptosis by cellular acidosis (1). Figure 1 shows the complex pathways involved in solid tumour development. There are two major growth phases: the pre-clinical growth phase without angiogenesis and the clinical rapid growth phase with angiogenesis. In both cases, hypoxic glycolysis is activated and produces a large amount of acid metabolites. The subsequent decrease in intracellular pH has been shown to reduce DNA repair activity,

Correspondence to: K. Kohno, Department of Molecular Biology, University of Occupational and Environmental Health, School of medicine, 1-1 Iseigaoka Yahatanishi-ku Kitakyushu, Fukuoka 807-8555, Japan. Tel.: +81-93-691-7423; Fax: +81-93-692-2766; E-mail: k-kohno@med.uoeh-u.ac.jp
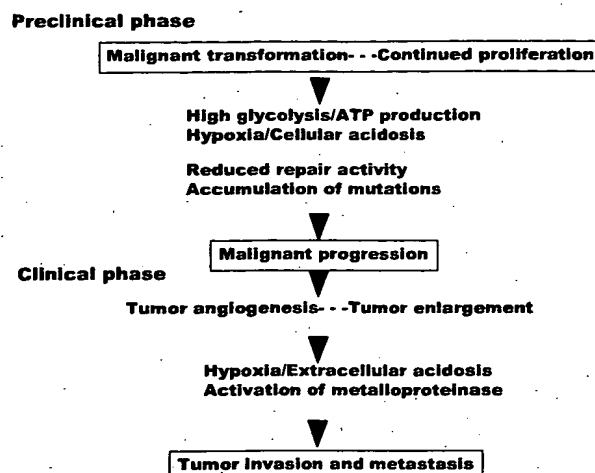
**Preclinical phase**

| Malignant transformation- - -Continued proliferation |

▼

High glycolysis/ATP production
Hypoxia/Cellular acidosis

Reduced repair activity
Accumulation of mutations

▼

| Malignant progression |

**Clinical phase**               ▼

Tumor angiogenesis- - -Tumor enlargement

▼

Hypoxia/Extracellular acidosis
Activation of metalloproteinase

▼

| Tumor invasion and metastasis |

**Figure I**   Development of a solid tumour. Serial biological events during solid tumour development are shown.



**Figure 2**   Structure of V-ATPase. ATP hydrolysis by the VI domain drives proton transport through the membrane-integrated VO domain.

indicating that spontaneous mutations are accumulated following malignant progression of solid tumours (2,3). Malignant progression is accompanied by novel gene expression (4–6) and a change in the DNA methylation status (7). Rapid tumour growth with angiogenesis induces extracellular acidosis, which in turn leads to activation of metalloproteinases (8). Thus, solid tumours attain the ability to invade tissues and to metastasize. Maintenance of pH homeostasis is crucial for solid tumour development, thus tumour cells express various pH regulators to avoid apoptosis.

## PROTON PUMP

The vacuolar proton pump (V-ATPase) belongs to a class of pumps that includes the F-ATPase (energy-coupling factors). The V-ATPase is composed of two multi-subunit sectors, the V0 and V1 domains, as shown in Figure 2. Table 1 shows the molecular mass, subunit function and human genes encoding each subunit. The V-ATPase is expressed in eukaryotes from yeast to man (9). It is present not only in the membrane of organelles, but also in the plasma membrane. The V-ATPase pumps protons from the cytoplasm to the lumen of vacuoles or into the extracellular space using the energy produced by ATP hydrolysis. A significant feature of V-ATPase is the wide variety of cellular functions that it is involved in (see Table 2). The V-ATPase is involved in both endocytosis and intracellular transport. In receptor-mediated endocytosis, the dissociation of the ligand–receptor complex is initiated in acidic endosomes. After dissociation, receptors recycle to the
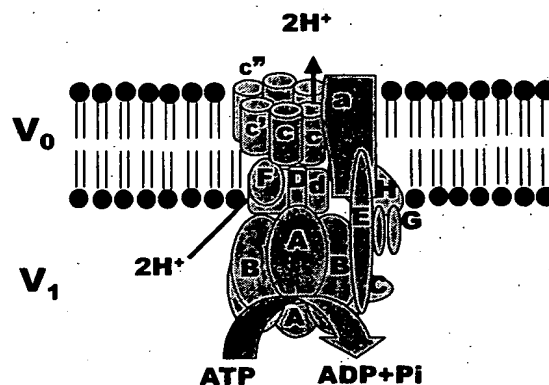
plasma membrane. After the targeting of newly synthesized lysozomal enzymes from the Golgi to lysozomes, lysozomal enzymes are released from the mannose-6-phosphate receptor by the acidification of endosomes. Mutations in the genes encoding the B and A subunits cause human diseases such as renal tubular acidification, sensorineural deafness and malignant osteopetrosis. It appears that some isoforms show tissue-restricted expression. Thus, plasma membrane V-ATPase has important roles in renal acidification, pH maintenance in mechanosensory hair cells and bone resorption. β1 integrin is involved in cell migration, proliferation, differentiation, cytoskeletal organization, signal transduction and cell sensitivity to anticancer agents. It binds to the c subunit on the last of four trans-membrane helices. Over-expression of the c subunit or expression of a subunit c with the fourth helix deleted alters the morphology of myoblasts and fibroblasts (10). Thus, interactions of the c subunit with β1 integrin are important for cell growth control. Recently, the c subunit has been reported to suppress β1, 6 branching N-linked oligosaccharides of β1 integrin and epidermal growth factor (EGF): this ability to influence glycosylation is located in the second and fourth helices. However, the effect of the c subunit on glycosylation is independent of its binding to β1 integrin (11).

The E subunit of V-ATPase interacts with the Db1 oncoprotein homology domain of mSos-1, which has a dual role in activating Ras and Rac1. This observation suggests that the E subunit may participate in regulation of the mSos-1-dependent Rac1 signaling pathway involved in growth factor-mediated cell growth control (12). Many tumour cells secrete lysosomal enzymes that degrade the extracellular matrix. The activity of these enzymes is markedly enhanced in an acidic extracellular environment.

**TABLE I** Function and subunit composition of the vacuolar proton pump (V-ATPase)

| Domain | Subunit | Gene | Chromosome | M.W. (kDa) | Function | Interacting protein |
|--------|---------|------|------------|------------|----------|---------------------|
| VI | A | ATP6AI | 3p13 | 70 to 73 | ATP hydrosis | |
| | | ATP6A2 | ?. | ? | | |
| | B | ATP6BI | 2cen | 56 to 58 | ATP binding | |
| | | ATP6B2 | 8p21 | | | |
| | C | ATP6C | 8p22 | 40 to 42. | | |
| | D | ATP6M | 14 | 34 | | |
| | E | ATP6E | 22q11 | 31 to 33 | | Aldolase, Sos |
| | F | ATP6SI4 | 12 | 14 | | |
| | G | ATP6G | 6p21 | 13 to 15 | | |
| | H | N.C. | ? | 50 to 54 | | |
| VO | a | ATP6N | 17q21 | 100 to 116 | Proton translocation Bafilomycin binding | |
| | c | ATP6L | 16p13 | 17 | | Integrin β1 |
| | c' | N.C. | ? | 17 | | |
| | c" | ATP6F | 1p32 | 19 | | |
| | d | ATP6N2 | ? | 38 | | |

N.C., not cloned.

**TABLE 2** Functions of V-ATPase

| | |
|---|---|
| 1. | Endocytosis |
| 2. | Intracellular transport |
| 3. | Cytoplasmic pH homeostasis |
| 4. | Bone resorption |
| 5. | Tumour metastasis |

Thus, the plasma membrane V-ATPase is involved in tumour invasion/metastasis and is thought to be a potential target in cancer therapy. The V-ATPase has been shown to be over-expressed in multidrug-resistant cells (13) and furthermore, altered cytosolic pH has been implicated in drug resistance (14,15). Cells with multidrug resistance contain more acidic organelles than drug-sensitive parental cells, suggesting that acidic organelles are related to the observed resistance. Daunomycin and some anticancer agents such as doxorubicin and vinblastine have been found to accumulate in acidic organelles. In cells with multidrug resistance, these agents are then removed from the cell via exocytosis (16). This accumulation was sensitive to bafilomycin A1, an inhibitor of V-ATPase, but was insensitive to other transporter inhibitors and P-glycoprotein inhibitors (17–19). Recently, it has been shown that V-ATPase is up-regulated in cisplatin-resistant cells. Cellular pH is higher in cisplatin-resistant cells than in drug-sensitive cells (13). In addition cisplatin-DNA adduct formation is enhanced under acidic conditions and by a low chloride concentration. We hypothesize that cisplatin-resistant cells may increase intracellular pH by induction of the V-ATPase subunit genes, thus avoiding the cytotoxicity of cisplatin. Intracellular pH in cisplatin-resistant cells is higher than in sensitive parental cells due to up-regulation of V-ATPase subunit genes. DNA–cisplatin cross-links appear to form well under acidic conditions, thus a reduced intracellular pH is associated with increased sensitivity to cisplatin.

Recently, ionizing radiation has been reported to induce development of acidic vesicular organelles in neoplastic epithelial cells (20). Interference with acidification of vesicular organelles by bafilomycin A1, results in increased radio-sensitivity. Another report suggests that bafilomycin A1-treated cells show increased accumulation of p53 protein and p53-dependent trans-activation of gene expression (21). Inhibitors of V-ATPase may produce a supra-additive effect with other anticancer agents or irradiation. Thus, tumour pH is important in governing the response of cancer cells to irradiation, hyperthermia and chemotherapy. Recently, it has been shown that V-ATPase inhibitors induce EGF-dependent apoptosis in A431 cells. In addition intracellular signal transduction induced by the EGF/EGFR complex is blocked by V-ATPase inhibitors. These results indicate that V-ATPase inhibition may be a potential target for cancer chemotherapy.

The anticancer agent TAS-103 induces apoptosis by causing cellular acidosis. TAS-103 can up-regulate the cellular expression of proton pump genes. The proton pump inhibitor, bafilomycin A1, can enhance TAS-103-induced apoptosis (22). Intracellular acidification, an early event in apoptosis, increases the susceptibility of cells to killing by chemotherapeutic agents and has been found in HL-60 cells undergoing apoptosis in response to etoposide and camptothecin (23,24). This indicates that intracellular acidification activates endonucleases,

inducing cellular DNA fragmentation (25). These results indicate that V-ATPase inhibits apoptosis of cancer cells by preventing cellular acidosis and further, that V-ATPase inhibitors, in combination with low-dose anticancer agents, may provide a new therapeutic approach.

Several inhibitors have been found to interact with V-ATPase, interfering with both ATP hydrolysis and proton translocation activities (Table 3A). Inhibitors can be divided into two classes: soluble-domain inhibitors and inhibitors acting at membrane sites. At low micromolar concentrations,

soluble-domain inhibitors, such as N-ethylmaleimide (NEM) and 7-chloro-4-nitrobenzo-2-oxa-1,3-diazole chloride (NBD-Cl) effectively inhibit ATP hydrolysis (26). Inhibitors acting at membrane sites such as dicyclohexyl-carbodiimide (DCCD), inhibit the c subunit of V-ATPase (26,27). Bafilomycin A1 or concanamycin A (macrocyclic lactone class) at nanomolar concentrations selectively inhibit V-ATPase and also inhibit growth and induce apoptosis in various human cell lines (28–31). The cyclohexadepsipeptide, destruxin, which is a mycotoxin, has been demonstrated to be a highly specific inhibitor

**TABLE 3**  Inhibitors of pH regulators

A. V-ATPase inhibitors
  Bafilomycin A1
  Concanamycin A (Folimycin)/B
  NEM: N-ethyl-maleimide
  NBD-Cl: 7-chloro-4-nitrobenzo-2-oxa-1,3-diazole
  DCCD: N,N'-dicyclohexyl-carbodiimide
  Destruxin B
  Salicylihalamide A
  Lobatamide
  Oximidine

B. NHE inhibitors
Guanidine derivatives
  (i) Benzoylguanidine
    Cariporide, HOE642: 4-isopropyl-3-methylsulphonylbenzoyl-guanidine methanesulphonate
    Hoe 694: 3-methylsulfonyl-4-piperidinobenzoyl, guanidine hydrochloride
    FR183998: 5-(2,5-dichlorothiophen-3-yl)-3-[(2-dimethylaminoethyl)carbamoyl]benzoylguanidine dihydrochloride
    FR168888: 5-hydroxymethyl-3-(pyrrol-1-yl) benzoylguanidine methanesulfonate
    EMD 85131: 2-methyl-5-methylsulfonyl-1-(1-pyrrollyl)-benzoylguanidine
  (ii) Carbonylguanidine
    Zoniporide or CP-597,396: [1-(Quinolin-5-yl)-5-cyclopropyl-1H-pyrazole-4-carbonyl]guanidine hydrochloride monohydrate
    TY-12533: 6,7,8,9-tetrahydro-2-methyl-5H-cyclohepta[b]pyridine-3-carbonylguanidine maleate
    CAS 181048-29-3, MS-31-050: 2-(2-methylphenyl)-5,7-dimethoxy-4-quinolyl carbonylguanidine dihydrochloride
    CAS 181048-36-2, MS-31-038: 2-phenyl-8-(2-methoxyethoxy)-4-quinolyl carbonylguanidine bismethanesulfonate
    KB-R9032: N-(4-isopropyl-2,2-dimethyl-3-oxo-3,4-dihydro-2H-benzo[1,4]oxazine-6-car bonyl)guanidine (4b) methanesulfonate salt
  (iii) Others
    T-162559: (5E,7S)-[7-(5-fluoro-2-methylphenyl)-4-methyl-7,8-dihydro-5(6H)-quinolinylideneamino] guanidine dimethanesulphonate

Amiloride derivatives
  DMA: 5'-(N,N-dimethyl)-amiloride
  HMA: 5-(N,N-hexamethylene) amiloride
  MIA: 5-(N-ethyl-N-isopropyl)-amiloride

C. Bicarbonate transporter inhibitor
  Triflocin: 4-(α,α,α-trifluoro-m-toluidino)-nicotinic acid
  DIDS: 4,4'-diisothiocyanato-stilbene-2,2'-disulfonic acid
  SITS: 4-acetamido-4'-isothiocyanostilbene-2,2'-disulfonic acid
  S3705

D. MCT inhibitors
  DIDS: 4,4'-diisothiocyanato-stilbene-2,2'-disulfonic acid
  α-cyano-4-hydroxycinnamate (α-CHC)
  p-Chloromercuribenzenesulphonate
  Diethyl pyrocarbonate
  Quercetin

of the V-ATPase. Recently described specific inhibitors of mammalian V-ATPase belonging to the benzolactone enamide class, such as salicylihalamide, lobatamides and oximidines appear promising as anticancer agents. Among these agents, salicylihalamide A can discriminate between mammalian and non-mammalian V-ATPases. The next step is to discover the mode of action of salicylihalamides in human cells.

V-ATPase genes are considered to be "housekeeping genes" which is strongly regulated in response to growth rate. We have isolated and characterized several genomic clones containing the 5' end of human V-ATPase genes. The promoters of five V-ATPase genes encoding A1, C, E, c and c" subunits were examined with regard to their structure and transcription factor binding sites. These promoters exhibited a GC-rich region in the area of the first exon and lacked TATA and CCAAT boxes. We found putative Sp1 binding sites in their promoter regions, which are also frequently found in mammalian housekeeping genes. We have shown that cooperative binding of Sp1 and Oct1 to the promoter region of c subunit is required for basal expression and promoter activation by anticancer agents (22). Molecular mechanisms of transcription relevant to the other subunits encoded by multiple V-ATPase genes remain to be elucidated. It will be of considerable interest to identify the transcription factors that regulate the V-ATPase subunit genes in cancer cells.

## SODIUM/PROTON EXCHANGER

Proton fluxes across plasma membranes are regulated by several families of ion exchangers, including the sodium/proton exchanger (NHE). Seven NHE family members have been identified, as shown in Table 4. In humans, NHEs are comprised of 669–896 amino acids and are predicted to consist of 12 transmembrane segments with cytoplasmic N- and C-terminal domains, Figure 3. The cytoplasmic domain of an NHE contains the pH sensor and maintenance

sites. Among this family, NHE1 is ubiquitously expressed and plays a critical role in intracellular pH and cell volume homeostasis (32). Cell proliferation is associated with the expression of NHE1, since mitogens induce intracellular alkalinization. Cells lacking NHE activity show markedly impaired proliferation. This has been shown clearly in NHE-deficient mutant cells derived from a human bladder cancer cell line, isolated using the proton suicide selection method (33). NHE-deficient cells have an increased cell volume relative to parental cells and show acid-sensitive growth. Furthermore, NHE-deficient cells showed either a lost or severely reduced capacity for tumour growth in vivo, indicating that NHE activity is important for tumour growth. However, the molecular mechanism of proliferation regulated by NHE1 remains unclear.

It has been shown that NHE-dependent intracellular alkalinization occurs early in malignant transformation and plays an essential role in the development of malignant progression (34). NHE1 is also involved in cell survival and has anti-apoptotic activity. Cellular acidosis and a decrease in cell volume are both triggers of apoptosis (35). Furthermore, the activation of Fas receptors inhibits NHE1 activity (36). The cytoplasmic domain contains the region that is activated when growth factors and mitogens act on the cell surface. Phosphorylation of this region plays an essential role in the activity of NHE1. Activation of NHE1 by phosphorylation has been shown to abrogate both intracellular acidification and cell shrinkage. In addition, stress-activated p38 mitogen-activated protein kinase (MAPK) phosphorylates the C-terminal domain of NHE1 (37). Important questions remain to be answered, however, as to whether phosphorylation status is associated with the growth rate of solid tumours in vivo. Various structural and regulatory proteins interact with the long intracellular C-terminal domain and these interactions modulate NHE activity resulting in changes in cellular morphology, adhesion and migration.

Recently, the ezrin, radixin, moesin (ERM) family of proteins has been shown to interact with NHE1

**TABLE 4**  Characteristics of NHE isoforms

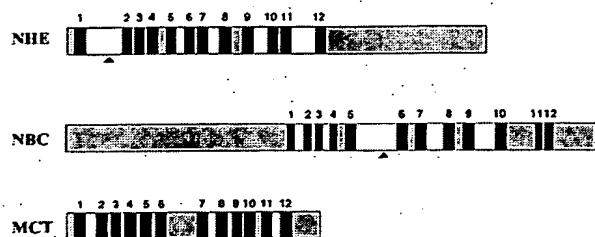| NHE isoform | AA | Chromosome | Tissue distribution | Accession No. |
|---|---|---|---|---|
| NHE1 | 815 | 1 | Ubiquitous | S68616 |
| NHE2 | 812 | 2 | Kidney/GI tract | AF073299 |
| NHE3 | 834 | 5 | Kidney/GI tract | NM_004174 |
| NHE4 | ? | (2) | Kidney/GI tract | N.C. |
| NHE5 | 896 | 16 | Brain | AF111173 |
| NHE6 | 669 | X | Mitochondria | AF030409 |
| NHE7 | 725 | X | TGN | AF298591 |

N.C., not cloned.

**Figure 3** Schematic structures of three pH regulators. All members have internal N- and C-terminal domains as indicated in grey. Black boxes indicate the proposed position of *trans*-membrane domains, shown by numbering. Arrowheads indicate glycosylaton sites.

(38). The ERM proteins are also known to interact with the adhesion molecule, CD44, which is ubiquitously expressed in cancer cells and regulates cell adhesion and motility (39,40). Various molecules involved in signal transduction regulate NHE1 activity, such as Ras-mediated ERK, G protein-coupled receptors, PKC, RhoA, and integrin receptors (41–46). The formation of tumour cell pseudopodia is also regulated by NHE1 via their interaction with molecules involved in the actin cytoskeleton. However, further study of the biological roles of the NHE family in cancer cells is required to fully explore the therapeutic potential of any inhibitors.

Two classes of NHE inhibitor have been identified to date. The first is amiloride and its derivatives and the second is guamidine and its derivatives (see Table 3B). Amiloride has been shown to non-specifically inhibit all NHE isoforms. In contrast, benzoylguamidine is an efficient and selective inhibitor of NHE1. Among these agents, zoniporide appears to have therapeutic potential as a cardioprotective agent. Recently, amiloride derivatives have been shown to induce apoptosis in leukemic cells. Furthermore, there appears to be a difference in the sensitivity of normal and leukemic cells to these agents, indicating that NHE1 inhibitors may have potential as anti-leukemic agents.

## BICARBONATE TRANSPORTERS

The mammalian bicarbonate transporter (BCT) superfamily is categorized into two families: (i) family members of the solute carrier 4 (SLC4), such as sodium bicarbonate co-transporters (NBCs 1–4) (47), sodium-dependent $Cl^-/HCO_3^-$ exchanger (NCBE) and anion exchangers (AE 1–4), and (ii) some family members of the solute carrier 26 (SLC26). Table 5 summarizes the BCT families and their tissue distribution. NBCs are comprised of 1018–1137 amino acids and are predicted to consist of 12 *trans*-membrane segments with cytoplasmic N- and C-terminal domains, Figure 3. The N-terminal domain is extremely long, indicating that various molecules may interact with the NBC via the N-terminal domain. The NBC is responsible for the transport of bicarbonate from the blood to the cell. NBC1 is mainly expressed in pancreatic duct cells and is activated by the cystic fibrosis *trans*-membrane conductance regulator. NBC2 and NBC3 are expressed in a variety of cells and are involved in cellular pH regulation. Very little information is available about their expression in cancer cells. Our preliminary data indicates that NBC2 is significantly expressed in cancer cells, whereas NBC1 is not (unpublished data). Interestingly, the von Hippel–Lindau tumour suppressor has been shown to regulate the activity of AE and NHE in renal cancer (48). Further studies are needed to establish the potential roles of BCTs in tumour cells.

It is well known that both 4,4'-diisothiocyanato-stilbene-2,2'-disulfonic acid (DIDS) and 4-acetamido-4';isothiocyanostilbene-2,2'-disulfonic acid (SITS) non-specifically inhibit the activity of members of the BCT family (Table 3C). However, there are few selective inhibitors of the BCT family. Triflocin can inhibit the $Na-HCO_3$ symport in the proximal tube (49). Recently, S3705 has been shown to inhibit NCBE activity and tumour growth when cells were incubated at low extracellular pH (50).

**TABLE 5** Characteristics of BCT family

| BCT family | AA | Chromosome | Tissue distribution | Accession No. |
|---|---|---|---|---|
| NBCI | 1035 | 4q21 | Kidney/pancreas Liver/GI tract | NM_003759 |
| NBC2 | 1018 | 3q21 | Retina/muscle | NM_003615 |
| NBC3 | 1044 | 12 | Brain/kidney | NM_004858 |
| NBC4 | 1137 | 2p13 | Ubiquitous | NM_021196 |
| NCBE | 1088 | 2q23 | Brain/kidney | NM_002058 |
| AEI | 911 | 17q21 | Erythrocyte | NM_000342 |
| AE2 | 1241 | 7q35 | Ubiquitous | NM_003040 |
| AE3 | 1232 | 2q36 | GI tract | NM_005070 |
| AE4 | 983 | 5 | ? | XM_038736 |

## MONOCARBOXYLATE TRANSPORTERS

MCT play a central role in cellular metabolism (51) and are essential for transport monocarboxylates, such as lactate, across the plasma membrane. Several MCTs have been cloned and are known to belong to a new transporter family. Table 6 summarizes the chromosome localization and tissue distribution of the human MCT family. The predicted topology indicates that the number of *trans*-membrane domains is 12 with the N- and C-termini located within the cytoplasm, Figure 3. The *trans*-membrane helix topology is shared with other plasma membrane transporters, such as glucose transporters. Both MCT1 and MCT4 are often expressed in cancer cells and are closely associated with CD147, otherwise known as Extracellular Matrix Metalloproteinase Inducer. CD147 is highly expressed in human cancer cells and induces matrix metalloproteinase production, facilitating tumour cell invasion (52). However, a high concentration of lactate in tumour tissue is closely associated with metastasis and poor patient survival (53).

Under hypoxic conditions in tumour tissue, accumulation of lactate and a decrease in pH have been shown to cause apoptosis (54,55). To counter apoptosis caused by lactic acidosis, MCTs may be up-regulated in highly proliferative tumours. Overall, it seems that expression of MCTs may be associated with invasion, metastasis and a poor prognosis. Hypoxia is known to up-regulate the expression of lactate dehydrogenase and vascular endothelial cell growth factor, a well-known transcriptional mechanism, involving hypoxia inducible factor 1 and hypoxia responsible element. The distribution of lactate dehydrogenase is similar to that of MCT4 in muscle fiber, suggesting that the MCT4 gene may be one of the hypoxia-inducible genes. The levels of MCT1 mRNA and protein have been shown to be significantly reduced in colonic adenomas and carcinomas, especially in poorly differentiated carcinomas. Conversely, a reduction in MCT1 expression is accompanied by the expression of the high affinity glucose transporter, GLUT1 (56) and a down-regulation of the low affinity glucose transporter, GLUT2 (57). Interestingly, the MCT4 protein was not observed, although MCT4 mRNA was detected in colon carcinoma. Further experimentation is needed to fully understand the exact expression and roles of MCTs in human cancer.

Inhibitors of MCT may be categorized into four classes, (1) aromatic monocarboxylates, (2) inhibitors of anion transport, (3) bioflavenoids and (4) others (see Table 3D).

## PROSPECTS

In general, intracellular pH is similar in both solid tumour and normal tissues. However, extracellular pH is higher in normal tissue and lower in solid tumours. Thus there is a difference in the cellular pH gradient between the two tissues. The expression profile of pH regulators is also different in tumour and normal tissues. It has been shown that intracellular accumulation of various lipophilic anticancer agents is modulated by the cellular pH gradient. Thus, this difference in pH gradients may provide the basis for selective cancer chemotherapy (58,59).

During the 1990s, most of the currently known human pH regulators were cloned. A great deal of work is needed, however, to analyze the functional properties of each pH regulator in physiological pH homeostasis. It has been proposed that regulation of intracellular pH may be a possible mechanism for tumour-selective therapy (60–62). The past decade has also seen the discovery of the physiological mechanism by which a decrease in intracellular pH is the initial trigger for a cascade of events resulting in apoptosis. It is still unclear, however, which pH regulators are expressed and function as anti-apoptotic factors by preventing cellular acidosis in tumour tissue. Whether there is functional redundancy amongst these pH regulators also remains unclear. Some of these questions will be answered by

**TABLE 6** Characteristics of MCT isoforms

| MCT isoform | AA | Chromosome | Tissue distribution | Accession No. |
|---|---|---|---|---|
| MCT1 | 494 | 1p12-13 | Brain/heart/colon/RBC | L31801 |
| MCT2 | 478 | 12q13 | Liver/testis | AF049608 |
| MCT3 | 504 | 22q12-13 | Retina | AL031587 |
| MCT4 | 465 | 17 | Skeletal muscle | U81800 |
| MCT5 | 487 | 1p36 | Placenta | U59185 |
| MCT6 | 505 | 17q12 | Kidney/placenta | U59299 |
| MCT7 | 523 | ? | Pancreas | U79745 |
| MCT8 | 613 | Xq13 | Liver/kidney/heart | U05315 |
| MCT9 | ? | 10 | ? | N.C. |

N.C. not cloned.

profiling the expression of the pH regulators in solid tumours. Development of useful therapeutic agents for selective inhibition of pH regulators remains a final goal. Overall, these issues clearly require further extensive investigation to provide an answer to the enduring question of how important control of tumour pH is for cancer therapy.

## ACKNOWLEDGEMENTS

## REFERENCES

1. Vaupel P, Kallinowski F, Okunieff P. Blood flow, oxygen and nutrient supply, and metabolic microenvironment of human tumours: review. Cancer Res 1989; 49: 6449–6465.
2. Yuan J, Narayanan L, Rockwell S, et al. Diminished DNA repair and elevated mutagenesis in mammalian cells exposed to hypoxia and low pH. Cancer Res 2000; 60: 4372–4376.
3. Kondo A, Safaei R, Mishima M, et al. Hypoxia-induced enrichment and mutagenesis of cells that have lost DNA mismatch repair. Cancer Res 2001; 61: 7603–7607.
4. Hanahan D, Christofori G, et al. Transgenic mouse models of tumour angiogenesis: the angiogenic switch, its molecular controls, and prospects for preclinical therapeutic models: review. Eur J Cancer 1996; 32A: 2386–2393.
5. Hanahan D, Folkman J. Patterns and emerging mechanisms of the angiogenic switch during tumourigenesis: review. Cell 1996; 86: 353–364.
6. Hanahan D, Weinberg RA. The hallmarks of cancer. Cell 2000; 100: 57–70.
7. Widschwendter M, Jones PA. DNA methylation and breast carcinogenesis: review. Oncogene 2002; 21: 5462–5482.
8. Egeblad M, Werb Z. New functions for the matrix metalloproteinases in cancer progression: review. Nat Rev Cancer 2002; 2: 161–174.
9. Nishi T, Forgac M. The vacuolar (H+)–ATPases-nature's most versatile proton pumps: review. Nat Rev Mol Cell Biol 2002; 3: 94–103.
10. Skinner MA, Wildeman AG. β1 integrin binds the 16-kDa subunit of vacuolar H+-ATPae at a site important for human papillomavirus E5 and platelet-derived growth factor signaling. J Biol Chem 1999; 274: 23119–23127.
11. Skinner MA, Wildeman AG. Suppression of tumour-related glycosylation of cell surface receptors by the 16-kDa membrane subunit of vacuolar H+-ATPase. J Biol Chem 2001; 276: 48451–48457.
12. Miura K, Miyazawa S, et al. The Sos1-Rac1 signaling: possible involvement of a vacuolar H+–ATPase E subunit. J Biol Chem 2001; 276: 46276–46283.
13. Murakami T, Shibuya I, Ise T, et al. Elevated expression of vacuolar proton pump genes and cellular pH in cisplatin resistance. Int J Cancer 2001; 93: 869–874.
14. Beck WT. The cell biology of multiple drug resistance. Biochem Pharmacol 1987; 36: 2879–2887.
15. Moriyama Y. Membrane energization by proton pumps is important for compartmentalization of drugs and toxins: a new type of active transport. J Exp Biol 1996; 199: 1447–1454.
16. Willingham MC, Cornwell MM, Cardarelli CO, et al. Single cell analysis of daunomycin uptake and efflux in multidrug-resistant and -sensitive KB cells: effects of verapamil and other drugs. Cancer Res 1986; 46: 5941–5946.
17. Marquardt D, Center MS. Involvement of vacuolar H+–adenosine triphosphatase activity in multidrug resistance in HL60 cells. J Natl Cancer Inst 1991; 83: 1098–1102.
18. Martinez-Zaguilan R, Raghunand N, Lynch RM, et al. pH and drug resistance. I. Functional expression of plasmalemmal V-type H+–ATPase in drug-resistant human breast carcinoma cell lines. Biochem Pharmacol 1999; 57: 1037–1046.
19. Raghunand N, Martinez-Zaguilan R, Wright SH, et al. pH and drug resistance. II. Turnover of acidic vesicles and resistance to weakly basic chemotherapeutic drugs. Biochem Pharmacol 1999; 57: 1047–1058.
20. Paglin S, Hollister T, Delohery T, et al. A novel response of cancer cells to radiation involves autophagy and formation of acidic vesicles. Cancer Res 2001; 61: 439–444.
21. Long X, Crow MT, Sollott SJ, et al. Enhanced expression of p53 and apoptosis induced by blockade of the vacuolar proton ATPase in cardiomyocytes. J Clin Invest 1998; 101: 1453–1461.
22. Torigoe T, Izumi H, Ishiguchi H, et al. Enhanced expression of the human vacuolar H+–ATPase c subunit gene (ATP6L) in response to anticancer agents. J Biol Chem 2002; 277: 36534–36543.
23. Barry MA, Reynolds JE, Eastman A. Etoposide-induced apoptosis in human HL-60 cells is associated with intracellular acidification. Cancer Res 1993; 53: 2349–2357.
24. Goossens JF, Henichart JP, Dassonneville L, et al. Relation between intracellular acidification and camptothecin-induced apoptosis in leukemia cells. Eur J Pharm Sci 2000; 10: 125–131.
25. Sethi T, Rintoul RC, Moore SM, et al. Extracellular matrix proteins protect small cell lung cancer cells against apoptosis: a mechanism for small cell lung cancer growth and drug resistance in vivo. Nat Med 1999; 5: 662–668.
26. Forgac M. Structure and function of the vacuolar class of ATP-driven proton pumps. Physiol Rev 1989; 69: 765–796.
27. Finbow ME, Eliopoulos EE, Jackson PJ, et al. Structure of a 16 kDa integral membrane protein that has identity to the putative proton channel of the vacuolar H+–ATPase. Protein Eng 1992; 5: 7–15.
28. Bowman EJ, Siebers A, Altendorf K. Bafilomycins: a class of inhibitors of membrane ATPases from microorganisms, animal cells, and plant cells. Proc Natl Acad Sci USA 1988; 85: 7972–7976.
29. Zhang K, Wang ZQ, Gluck S. Identification and partial purification of a cytosolic activator of vacuolar H+–ATPases from mammalian kidney. J Biol Chem 1992; 267: 9701–9705.
30. Zhang K, Wang ZQ, Gluck S. A cytosolic inhibitor of vacuolar H+–ATPases from mammalian kidney. J Biol Chem 1992; 267: 14539–14542.
31. Drose S, Bindseil KU, Bowman EJ, et al. Inhibitiory effect of modified bafilomycins and concanamycins on P- and V-type adenosinetriphosphatases. Biochemistry 1993; 32: 3902–3906.
32. Putney LK, Denker SP, Barber DL. The changing face of the Na+/H+ exchanger, NHE1: structure, regulation, and cellular actions: review. Annu Rev Pharmacol Toxicol 2002; 42: 527–552.
33. Rotin D, Steele-Norwood D, Grinstein S, et al. Requirement of the Na+/H+ exchanger for tumour growth. Cancer Res 1989; 49: 205–211.
34. Reshkin SJ, Bellizzi A, Caldeira S, et al. Na+/H+ exchanger-dependent intracellular alkalinization is an early event in

malignant transformation and plays an essential role in the development of subsequent transformation-associated phenotypes. *FASEB J* 2000; 14: 2185–2197.

35. Lang F, Ritter M, Gamper N, et al. Cell volume in the regulation of cell proliferation and apoptotic cell death: review. *Cell Physiol Biochem* 2000; 10: 417–428.

36. Lang F, Madlung J, Bock J, et al. Inhibition of Jurkat-T-lymphocyte $Na^+/H^+$-exchanger by CD95 (Fas/Apo-1)-receptor stimulation. *Pflugers Arch* 2000; 440: 902–907.

37. Khaled AR, Moor AN, Li A, et al. Trophic factor withdrawal: p38 mitogen-activated protein kinase activates NHE1, which induces intracellular alkalinization. *Mol Cell Biol* 2001; 21: 7545–7557.

38. Denker SP, Huang DC, Orlowski J, et al. Direct binding of the Na–H exchanger NHE1 to ERM proteins regulates the cortical cytoskeleton and cell shape independently of $H^+$ translocation. *Mol Cell* 2000; 6: 1425–1436.

39. Yonemura S, Tsukita S, Tsukita S. Direct involvement of ezrin/radixin/moesin (ERM)-binding membrane proteins in the organization of microvilli in collaboration with activated ERM proteins. *J Cell Biol* 1999; 145: 1497–1509.

40. Goodison S, Urquidi V, Tarin D. CD44 cell adhesion molecules: review. *Mol Pathol* 1999; 52: 189–196.

41. Maly K, Hochleitner B, Uberall F, et al. Mechanism and biological significance of the Ha-ras-induced activation of the $Na^+/H^+$-antiporter. *Adv Enzyme Regul* 1990; 30: 63–74.

42. Bianchini L, L'Allemain G, Pouyssegur J. The p42/p44 mitogen-activated protein kinase cascade is determinant in mediating activation of the $Na^+/H^+$ exchanger (NHE1 isoform) in response to growth factors. *J Biol Chem* 1997; 272: 271–279.

43. Tominaga T, Ishizaki T, Narumiya S, et al. p160ROCK mediates RhoA activation of Na–H exchange. *EMBO J* 1998; 17: 4712–4722.

44. Tominaga T, Barber DL. Na–H exchange acts downstream of RhoA to regulate integrin-induced cell adhesion and spreading. *Mol Biol Cell* 1998; 9: 2287–2303.

45. Lehoux S, Ji A, Florian JA, et al. 14-3-3 binding to $Na^+/H^+$ exchanger isoform-1 is associated with serum-dependent activation of $Na^+/H^+$ exchange. *J Biol Chem* 2001; 276: 15794–15800.

46. Lagana A, Vadnais J, Le PU, et al. Regulation of the formation of tumour cell pseudopodia by the $Na^+/H^+$ exchanger NHE1. *J Cell Sci* 2000; 113: 3649–3662.

47. Soleimani M, Burnham CE. $Na^+:HCO_3^-$ cotransporters (NBC): cloning and characterization: review. *J Membr Biol* 2001; 183: 71–84.

48. Karumanchi SA, Jiang L, Knebelmann B, et al. VHL tumour suppressor regulates $Cl^-/HCO_3^-$ exchange and $Na^+/H^+$ exchange activities in renal carcinoma cells. *Physiol Genom* 2001; 5: 119–128.

49. Belachgar F, Hulin P, Anagnostopoulos T, et al. Triflocin, a novel inhibitor for the $Na–HCO_3$ symport in the proximal tubule. *Br J Pharmacol* 1994; 112: 465–470.

50. Wong P, Kleemann HW, Tannock IF. Cytostatic potential of novel agents that inhibit the regulation of intracellular pH. *Br J Cancer* 2002; 87: 238–245.

51. Halestrap AP, Price NT. The proton-linked monocarboxylate transporter (MCT) family: structure, function and regulation: review. *Biochem J* 1999; 343: 281–299.

52. Sun J, Hemler ME. Regulation of MMP-1 and MMP-2 production through CD147/extracellular matrix metalloproteinase inducer interactions. *Cancer Res* 2001; 61: 2276–2281.

53. Walenta S, Wetterling M, Lehrke M, et al. High lactate levels predict likelihood of metastases, tumour recurrence, and restricted patient survival in human cervical cancers. *Cancer Res* 2000; 60: 916–921.

54. Matsuyama S, Llopis J, Deveraux QL, et al. Changes in intramitochondrial and cytosolic pH: early events that modulate caspase activation during apoptosis. *Nat Cell Biol* 2000; 2: 318–325.

55. Park HJ, Lyons JC, Ohtsubo T, et al. Acidic environment causes apoptosis by increasing caspase activity. *Br J Cancer* 1999; 80: 1892–1897.

56. Lambert DW, Wood IS, Ellis A, et al. Molecular changes in the expression of human colonic nutrient transporters during the transition from normality to malignancy. *Br J Cancer* 2002; 86: 1262–1269.

57. Laybutt DR, Sharma A, Sgroi DC, et al. Genetic regulation of metabolic pathways in β-cells disrupted by hyperglycemia. *J Biol Chem* 2002; 277: 10912–10921.

58. Kozin SV, Gerweck LE. Cytotoxicity of weak electrolytes after the adaptation of cells to low pH: role of the transmembrane pH gradient. *Br J Cancer* 1998; 77: 1580–1585.

59. Gerweck LE, Seetharaman K. Cellular pH gradient in tumour versus normal tissue: potential exploitation for the treatment of cancer. *Cancer Res* 1996; 56: 1194–1198.

60. Lee AH, Tannock IF. Heterogeneity of intracellular pH and of mechanisms that regulate intracellular pH in populations of cultured cells. *Cancer Res* 1998; 58: 1901–1908.

61. Simon SM. Role of organelle pH in tumour cell biology and drug resistance. *Drug Discov Today* 1999; 4: 32–38.

62. Raghunand N, He X, van Sluis R, et al. Enhancement of chemotherapy by manipulation of tumour pH. *Br J Cancer* 1999; 80: 1005–1011.

# Enhanced Expression of the Human Vacuolar H+-ATPase c subunit Gene (ATP6L) in Response to Anticancer Agents*

Takayuki Torigoe‡§, Hiroto Izumi‡, Hiroshi Ishiguchi‡, Hidetaka Uramoto‡, Tadashi Murakami‡, Tomoko Ise‡, Yoichiro Yoshida‡§, Mizuho Tanabe‡, Minoru Nomoto‡, Hideaki Itoh§, and Kimitoshi Kohno‡¶

From the ‡Department of Molecular Biology and the §Department of Surgery 1, University of Occupational and Environmental Health, School of Medicine, 1-1 Iseigaoka, Yahatanishi-ku, Kitakyushu 807-8555, Japan

We have isolated two overlapping genomic clones that contain the 5'-terminal portion of the human vacuolar H+-ATPase c subunit (ATP6L) gene. The sequence preceding the transcription initiation site, which is GC-rich, contains four GC boxes and one Oct1-binding site, but there is no TATA box or CCAAT box. In vivo footprint analysis in human cancer cells shows that two GC boxes and the Oct1-binding site are occupied by Sp1 and Oct1, respectively. We show here that treatment with anticancer agents enhances ATP6L expression. Although cisplatin did not induce ATP6L promoter activity, it altered ATP6L mRNA stability. On the other hand, the DNA topoisomerase II inhibitor, TAS-103, strongly induced promoter activity, and this effect was completely eradicated when a mutation was introduced into the Oct1-binding site. Treatment with TAS-103 increased the levels of both Sp1/Sp3 and Oct1 in nuclear extracts. Cooperative binding of Sp1 and Oct1 to the promoter is required for promoter activation by TAS-103. Incubation of a labeled oligonucleotide probe encompassing the −73/−68 GC box and −64/−57 Oct1-binding site with a nuclear extract from drug-treated KB cells yielded higher levels of the specific DNA-protein complex than an extract of untreated cells. Thus, the two transcription factors, Sp1 and Oct1 interact, in an adaptive response to DNA damage, by up-regulating expression of the vacuolar H+-ATPase genes. Furthermore, combination of the vacuolar H+-ATPase (V-ATPase) inhibitor, bafilomycin A1, with TAS-103 enhanced apoptosis of KB cells with an associated increase in caspase-3 activity. Our data suggest that the induction of V-ATPase expression is an anti-apoptotic defense, and V-ATPase inhibitors in combination with low-dose anticancer agents may provide a new therapeutic approach.

Tumor cells possess high glycolytic activity, and rapid growth produces acidic metabolites. Moreover, tumor cells often exist in an hypoxic microenvironment lower in pH than that of surrounding normal cells. Hence, proton extrusion may be up-regulated to protect tumor cells from acidosis. Four major types of pH regulators have been identified in tumor cells as follows: sodium-proton exchangers, bicarbonate transporters, proton-lactate symporters, and proton pumps. The vacuolar H+-ATPase (V-ATPase)[1] is ubiquitously expressed in eukaryotic cells (1–6), not only in vacuolar membranes but also in plasma membrane (7–9). It is a multisubunit enzyme composed of a membrane sector and a cytosolic catalytic sector (10); it pumps protons from the cytoplasm to the lumen of the vacuole and also regulates cytosolic pH. V-ATPase is active in the plasma membrane of human tumor cells (11), and V-ATPase genes are considered "housekeeping genes." However, cytosolic pH is critical for the cytotoxicity of anticancer agents (12), and cellular acidosis is thought to be a trigger for apoptosis and to play a role in drug resistance. Therefore, understanding the mechanisms regulating tumor acidity is important for developing new approaches to cancer chemotherapy.

By using differential display, we have shown that one of the proton pump subunit genes, ATP6L (subunit c), is induced by cisplatin (13), and several V-ATPase subunit genes are up-regulated in drug-resistant cell lines (13, 14). Interaction of the V-ATPase c subunit with $\beta_1$ integrin has been reported (15, 16), and $\beta_1$ integrin-mediated signaling prevents lung cancer cells from drug-induced apoptosis. The level of the V-ATPase c subunit may be critical for V-ATPase activity. In order to study transcriptional regulation of the c subunit at the molecular level, we have identified its promoter sequences and characterized the transcription factors that regulate its expression in cancer cells. We hypothesized that V-ATPase expression is up-regulated in response to cellular acidosis and show that c subunit promoter activity is activated by treatment with anticancer agents, especially the DNA topoisomerase II inhibitor, TAS-103 (17, 18), which can induce cellular acidosis (19). We show also that the levels of two transcription factors, Sp1 and Oct1, increase in response to genotoxic stress and that V-ATPase inhibition strongly enhances TAS-103-induced apoptosis.

## MATERIALS AND METHODS

*Isolation of V-ATPase Subunit c (ATP6L) Genomic Clones and DNA Sequencing*—ATP6L genomic clones were isolated from a human placental genomic library in EMBL3 by screening with cDNA. All positive phage were mapped with EcoRI and SalI. Several genomic fragments were also used as hybridization probes to confirm the overlapping regions. Two genomic DNA fragments around the first exon were subcloned into pUC18 (Fermentas AB, Lithuania) and sequenced with an Automated sequencer 377 (PE Applied Biosystems).

*Primer Extension Analysis*—The primer, 5'-GTCACATGACCT-

[1] The abbreviations used are: V-ATPase, vacuolar H+-ATPase; DTT, dithiothreitol; PMSF, phenylmethylsulfonyl fluoride; EMSA, electrophoretic mobility shift assay; PBS, phosphate-buffered saline; nt, nucleotide; PIPES, 1,4-piperazinediethanesulfonic acid; DMS, dimethyl sulfate.

GGGCCCCG-3', derived from the first exon of *ATP6L*, was labeled at its 5' end and hybridized with poly(A) RNA from KB cells in 80% formamide, 0.4 M NaCl, 40 mM PIPES (pH 6.4), and 1 mM EDTA for 4 h at 52 °C. The primer-RNA hybrid was precipitated and resuspended in reverse transcriptase mixture (Invitrogen). After 1 h of incubation at 42 °C, the reaction was terminated by making the solution 20 mM in EDTA. The RNA was hydrolyzed with 0.125 M NaOH for 1 h at 65 °C, the reaction neutralized, and the extended DNA then precipitated with alcohol. The DNA was analyzed on a 7 M urea, 6% polyacrylamide gel to determine the size of the extended product. Sequencing reactions using the same primer were similarly analyzed.

*Cell Culture and Antibody*—Human epidermoid cancer KB cells (20), human prostate cancer PC3 cells (21), and human breast cancer MCF7 cells (22) were cultured in Eagle's minimal essential medium (Nissui Seiyaku Co., Tokyo, Japan) or Dulbecco's modified Eagle medium (Nissui Seiyaku Co., Tokyo, Japan) containing 10% fetal bovine serum, 0.292 mg/ml L-glutamine, 100 units/ml penicillin, and 100 μg/ml kanamycin. The anti-Sp1 (catalogue number sc-420 for supershift assay, sc-59 for chromatin immunoprecipitation assay, and Western blotting), anti-Sp3 (sc-644), anti-Oct1 (sc-232), and anti-Oct2 (sc-233) antibodies were purchased from Santa Cruz Biotechnology. Antiserum to V-ATPase subunit E was generated by multiple immunization of a New Zealand White rabbit with synthetic peptides as described (23). The sequence of the synthetic peptides is ALFGANANRKFLD.

*Northern Blot Analysis*—Total RNA from KB cells was isolated using Sepasol reagent (Nacalai Tesque, Kyoto, Japan). RNA samples (20 μg/lane) were separated on a 1% formaldehyde-agarose gel and transferred to a Hybond N+ filter (Amersham Biosciences) with 10× SSC. Prehybridization and hybridization were performed as described (24). For analysis of stability of V-ATPase subunit transcripts by cisplatin or TAS-103, KB cells were treated with actinomycin D (1 μg/ml) and cisplatin (10 μM) or TAS-103 (4 μM) for 6 h. Cisplatin was purchased from Sigma, and TAS-103 was kindly provided from Taiho Pharmaceutical Co., Ltd. (Tokyo, Japan).

*Separation of Membrane Fractions*—KB cells were treated with or without TAS-103 for 12 h. Briefly, cells were homogenized in 0.25 M sucrose, and the homogenates were centrifuged at 3,000 rpm for 10 min. The supernatant was centrifuged at 15,000 rpm for 30 min. The pellets were resuspended to 0.25 M sucrose. The resuspension was overlaid with 2.10 and 1.25 M sucrose cushions and centrifuged at 24,000 rpm for 12 h. The membrane fractions at the 0.25–1.25 M sucrose interface were collected and used for Western blotting.

*Immunoprecipitation Assay*—For metabolic labeling, KB cells in a 100-mm tissue culture dish were cultured in Dulbecco's methionine and cysteine-free modified Eagle's medium (Invitrogen) supplemented with 1% dialyzed fetal calf serum and were labeled with 50 μCi/ml [³⁵S]methionine and -cysteine labeling mixture (Amersham Biosciences) with or without 4 μM TAS-103 for 12 h. After washing the cells twice with ice-cold phosphate-buffered saline (PBS), cells were lysed in RIPA buffer (50 mM Tris-HCl (pH 7.5), 1 mM EDTA, 150 mM NaCl, 1% Nonidet P-40, 0.1% SDS, 0.5% sodium deoxycholate, 1 mM PMSF). After centrifugation at 3,000 rpm for 5 min at 4 °C, 2 mg of supernatant (cellular fraction) were incubated with antiserum to V-ATPase subunit E or preimmune binding to 15 μl of protein A/G-agarose. The mixtures were incubated for 12 h at 4 °C and washed three times with RIPA buffer. Immunoprecipitation samples and 1% of preimmunoprecipitation samples (input) were simultaneously separated on a 15 or 10% SDS-PAGE and autoradiography.

*Construction of ATP6L Promoter-Luciferase Reporter and Expression Plasmids*—The *Eco*RI and *Not*I fragment (nt −1627 to nt +194) of the *ATP6L* gene into the *Sma*I site of basic vector 2 (Nippon Gene, Tokyo) was designed pV-ATPase c Luc1. For the construction of deletion constructs, it was digested with *Pst*I (pV-ATPase c Luc2), *Bsh*TI (pV-ATPase c Luc6), and *Nar*I (pV-ATPase c Luc7). The digestion products were self-ligated. Other constructs (pV-ATPase c Luc3, -4, and -5) were constructed by PCR (Fig. 7A). The pV-ATPase c Luc3m1, Luc3m2, Luc3m3, Luc3SR, and Luc3–5bp were constructed by PCR-based method using mutated oligonucleotides (Figs. 7B and 9B). *ATP6E* genomic clones were isolated from a human placental genomic library, and the 5'-flanking region of the *ATP6E* (nt −715 to +132) gene was subcloned in basic vector 2 (pV-ATPase E Luc1). Sp1 cDNA (encoding amino acids 30 to C-terminal) was kindly provided by Dr. Robert Tjian (University of California, Berkeley), and the *Xho*I fragment added start codon at the N-terminal start codon was ligated in pcDNA3 vector (Amersham Biosciences). For expression plasmids, full-length cDNA fragments of human Sp3, Oct1, and Oct2 were generated by reverse transcription-PCR using total RNA from KB cells and cloned into the pcDNA3 vector. The following oligonucleotides were used for cDNA

constructions: Sp3, 5'-ATGGCTGCCTTGGACGTGGATAGC-3' and 5'-TTACTCCATTGTCTCATTTCCAGAAAC-3'; Oct1, 5'-ATGAACAATC-CGTCAGAAACCAGTAAACC-3' and 5'-TCACTGTGCCTTGGAGGCG-GTGGTGG-3'; Oct2, 5'-ATGGTTCACTCCAGCATGGGGGC-3' and 5'-TTACCCCGTGCTGGGGTTCAGG-3'.

*Transient Transfection*—Cells were seeded into 12-well tissue culture plates at a concentration of 4 × 10⁴ KB cells, PC3 cells, and MCF7 cells. On the following day, cells were transfected with 0.4 μg of luciferase reporter plasmid DNA using 2 μl of Superfect reagent (Qiagen, Germany) according to the manufacturer's instructions. The β-galactosidase reporter gene (pSV-β-gal, Nippon Gene, Tokyo) was co-transfected as an internal control. After transfection for 12 h, the cells were washed, incubated at 37 °C for 12 h in fresh medium or in medium containing either TAS-103 (4 μM) or cisplatin (10 μM), and then harvested. For co-transfection experiments with Sp1, Sp3, Oct1, and Oct2 expression plasmids, PC3 cells were transfected with 0.2 μg of luciferase reporter plasmid (pV-ATPase c Luc3) and 0.4 μg of expression plasmid. After transfection for 12 h, the cells were incubated at 37 °C for 24 h in fresh medium and then harvested.

*Luciferase Assay*—Lysed cells were assayed for luciferase activity using a Picagene kit (Toyoinki, Tokyo, Japan); the light intensity was measured for 15 s with a luminometer (Dynatech ML1500, JEOL, Japan). The β-galactosidase enzyme assay was performed according to the protocol of Promega.

*In Vivo Footprint*—KB cells and MCF7 cells were treated with dimethyl sulfate (DMS) *in vivo* (25). The extracted DNA was cleaved with 1 M piperidine at 90 °C for 30 min. As a control guanine ladder, naked genomic DNA from KB cells was reacted with DMS *in vitro* and cleaved with piperidine as described above. Ligation-mediated PCR was performed as described previously (25, 26). The nucleotide sequences of individual primers are as follows: 5'-GCCTGCAGCTTCACGCC-3' (−172 to −184) primer 1; 5'-CGCCGGGAACCCAACACCTGC-3' (−135 to −115) primer 2; 5'-CCGGGAACCCAACACCTGCAGACGACGC-3' (−133 to −106) primer 3 for analysis of the lower strand of the subunit c gene. Primers 1 and 2 were used for the first strand synthesis and PCR amplification, respectively. Primer 3 was labeled at the 5' end with [γ-³²P]ATP and used for final detection of the ladder.

*Chromatin Immunoprecipitation Assay*—Protein-DNA cross-linking was performed by incubating KB cells with formaldehyde at a final concentration of 1% for 10 min at room temperature. Cells were washed with PBS and collected by centrifugation at 1,200 rpm for 5 min. Cells were then lysed in buffer X (50 mM Tris-HCl (pH 8.0), 1 mM EDTA, 120 mM NaCl, 0.5% Nonidet P-40, 10% glycerol, and 1 mM PMSF) for 15 min on ice. The lysate was sonicated with 10 pulses of 10 s each at 50–60% of maximum power with a sonicator (Taitec, Tokyo, Japan) equipped with a microtip to reduce the chromatin fragments to average sizes of less than 500 bp. Soluble chromatin was precleared by addition of 10 mg of protein A-Sepharose. An aliquot of precleared chromatin containing 1 × 10⁶ cells was removed and used in the subsequent PCR analysis. The remainder of the chromatin was divided, with each having 1 × 10⁶ cells, and diluted with buffer X. Then protein-DNA was incubated with 2 μg of anti-Sp1, anti-Oct1 antibody, and normal rabbit IgG in a final volume of 800 μl overnight at 4 °C. Immune complexes were collected by incubation with 15 μl of protein A/G-agarose for 1 h at 4 °C. Protein A/G-agarose pellets were washed once with 1 ml of buffer X, once with high salt buffer X (50 mM Tris-HCl (pH 8.0), 1 mM EDTA, 500 mM NaCl, 0.5% Nonidet P-40, 10% glycerol, and 1 mM PMSF), once with LiCl buffer (10 mM Tris, 1 mM EDTA, 0.25 M LiCl, 1% Nonidet P-40, and 1% sodium deoxycholate (pH 8.0)), and twice with TE (10 mM Tris, 1 mM EDTA (pH 8.0)). Immune complexes were eluted twice with 250 μl of elution buffer (0.1 M NaHCO₃, 1% SDS). To reverse the protein-DNA cross-linking, eluted samples were incubated with 0.2 M NaCl for 4 h at 65 °C. Samples were digested with proteinase K (0.04 mg/ml) for 2 h at 45 °C and then with RNase A (0.02 mg/ml) for 30 min at 37 °C. DNA was purified with phenol/chloroform followed by ethanol precipitation. Purified DNA was resuspended in 20 μl of H₂O. Aliquots of 1 μl of serial dilution were analyzed by PCR with the appropriate primer pairs. The V-ATPase c promoter primers are as follows: 5'-CTGCAGACGACGCG-CAGCCGCAGAGGAGGC-3' and 5'-GCGCGAGACCGGTCCAACGCT-GCGGAGATC-3', and the *YB-1* promoter primers are 5'-AGATCTCT-ATCACGTGGCTGTTGC-3' and 5'-AAGCTTATCAGTCCTCCATTCTC-ATTGG-3'. Amplification was performed for a pre-determined optimal number of cycles. PCR products were separated by electrophoresis on 2% agarose gel, which were stained with ethidium bromide.

*Preparation of Nuclear Extracts*—Nuclear extracts using buffer S of KB cells were prepared as described (27). Briefly, 2 × 10⁷ cells were collected with PBS, resuspended in 1 ml of ice-cold 10 mM HEPES-KOH (pH 7.9), 1.5 mM MgCl₂, 10 mM KCl, 0.2 mM PMSF, 0.5 mM DTT, and

*ATP6L Gene Expression*

incubated on ice for 15 min. The cells were lysed with a dropping of 0.6% Nonidet P-40, and the lysate was centrifuged at 3,000 rpm for 10 min. The resulting nuclear pellets were resuspended in 50 μl of ice-cold buffer S (20 mM HEPES-KOH (pH 7.9), 25% glycerol, 1.5 mM MgCl$_2$, 10 mM KCl, 0.2 mM EDTA, 0.2 mM PMSF, and 0.5 mM DTT), and KCl was added to a final concentration of 0.4 M with frequent gentle mixing. Following centrifugation for 5 min at 4 °C in a microcentrifuge to remove insoluble material, the supernatant (nuclear extract) was stored at −70 °C. Nuclear extracts using buffer C were also prepared as described (28). Briefly, 2 × 10$^7$ cells were collected with PBS, resuspended in 1 ml of ice-cold 10 mM HEPES-KOH (pH 7.9), 10 mM KCl, 0.5 mM PMSF, 1 mM DTT, 0.1 mM EDTA, 0.1 mM EGTA, and incubated on ice for 15 min. The cells were lysed with a dropping of 0.6% Nonidet P-40, and the lysate was centrifuged at 3,000 rpm for 10 min. The resulting nuclear pellets were resuspended in 50 μl of ice-cold buffer C (20 mM HEPES-KOH (pH 7.9), 0.4 M NaCl, 1 mM EDTA, 1 mM EGTA, 1 mM PMSF, and 1 mM DTT) and incubated for 15 min on ice with frequent gentle mixing. Following centrifugation for 5 min at 4 °C in a microcentrifuge to remove insoluble material, the supernatant was stored at −70 °C. Its protein concentration was determined by the method of Bradford.

*EMSA*—EMSAs were performed as described (27). Briefly, 4 μg of nuclear extract proteins prepared with buffer S were incubated for 30 min at room temperature in a final volume of 20 μl containing 20 mM HEPES (pH 7.9), 1.5 mM MgCl$_2$, 0.2 mM EDTA, 0.1 mM PMSF, 1 mM DTT, 7.5% glycerol, 0.5 μg of poly(dI-dC), and 1 × 10$^4$ cpm (1 ng) of $^{32}$P-labeled oligonucleotide probe in the absence or presence of various competitors. On the other hand, 4 μg of nuclear extract proteins prepared with buffer C were incubated for 30 min at room temperature in a final volume of 20 μl containing 10 mM HEPES (pH 7.9), 50 mM NaCl, 1 mM MgCl$_2$, 1 mM EDTA, 1 mM DTT, 8% glycerol, 0.1 μg of poly(dI-dC), and 1 × 10$^4$ cpm (1 ng) of $^{32}$P-labeled oligonucleotide probe. Products were analyzed on nondenaturing 4% polyacrylamide gels using a bioimaging analyzer (BAS 2000; Fuji Photo Film, Tokyo). The sequences of oligonucleotides used for EMSAs are as follows: Oligo1 (−118 to −89), 5'-CTGCAGACGACGCGCAGCCGCAGAGGAGGC-3' and 3'-ACGTCT-GCTGCGCGTCGGCGTCTCCTCCGC-5'; Oligo2 (−98 to −69), 5'-CAG-AGGAGGCGGGGCGTCCGAGGCCCCGCC-3' and 3'-TCTCCTCCGC-CCCGCAGGCTCCGGGGCGGG-5'; Oligo3 (−78 to −49), 5'-AGGCCC-CGCCCCGTATGCTAATGAAGCACA-3' and 3'-CCGGGGCGGGGCA-TACGATTACTTCGTGTG-5'; Oligo4 (−58 to −29), 5'-ATGAAGCACA-CACCACACGCCCCCGCCCCG-3' and 3'-ACTTCGTGTGTGGTGTGG-CGGGGCGGGGCC-5'; Oligo5 (−38 to −9), 5'-CCCCGCCCCGGCGCG-AGACCGGTCCAACGC-3' and 3'-GGGCGGGGCCGCGCTCTGGCCA-GGTTGCGA-5'; Oligo6 (−28 to +2), 5'-GCGCGAGACCGGTCCAACG-CTGCGGAGATC-3' and 3'-GCGCTCTGGCCAGGTTGCGACGCCTCT-AGG-5'; Oligo3m1, 5'-AGGCCCTTCCCCGTATGCTAATGAAGCAC-A-3' and 3'-CCGGGAAGGGGCATACGATTACTTCGTGTG-5'; Oligo-3m2, 5'-AGGCCCCGCCCCGTATGCTTTTGAAGCACA-3' and 3'-CCG-GGGCGGGGCATACGAAAACTTCGTGTG-5'; Oligo3m3, 5'-AGGCCC-TTCCCCGTATGCTTTTGAAGCACA-3' and 3'-CCGGGAAGGGGCAT-ACGAAAACTTCGTGTG-5'; Oligo3SR, 5'-AGGGGGGCGGGGGTATG-CTAATGAAGCACA-3' and 3'-CCCCCCGCCCCCATACGATTACTTC-GTGTG-5'; Oligo3–5bp, 5'-AGGCCCCGCCCCGTCTAGAATGCTAAT-GAAGCACA-3' and 3'-CCGGGGCGGGGCAGATCTTACGATTACTTC-GTGTG-5'. For supershift assay, nuclear extracts were incubated with probes and 2 μg of anti-Sp1, anti-Sp3, anti-Oct1, and anti-Oct2 antibody for 30 min at 4 °C.

*Western Blotting*—Preparation of nuclear extracts and separation of membrane fractions were described above. Nuclear extracts (100 μg of protein) of KB cells prepared with buffer C were separated on a 10% SDS-PAGE, and membrane fractions (40 μg) by sucrose gradient of KB cells were separated on a 15% SDS-PAGE gel and transferred to polyvinylidene difluoride membrane (Millipore) using a semidry blotter. Prestained protein marker (Nacalai Tesque, Kyoto, Japan) was used as a molecular weight standard. Immunoblot analysis was performed with an appropriate dilution of each antibody.

*DNA Fragmentation*—KB cells in a 100-mm tissue culture dish were treated with TAS-103, bafilomycin A1 (Wako, Ohsaka, Japan), and a combination of these drugs for 36 h. The cells were washed twice with ice-cold PBS and then collected by centrifugation at 1,500 rpm for 10 min. The cell pellets were resuspended in 500 μl of Tris-EDTA buffer (20 mM Tris-HCl (pH 8.0), 20 mM EDTA) containing 0.1% SDS and proteinase K (0.5 mg/ml) at 50 °C for 2 h and then with RNase A (0.02 mg/ml) for 30 min at 37 °C. DNA was purified with phenol/chloroform followed by ethanol precipitation. Purified DNA was resuspended in 100 μl of H$_2$O. DNA samples were separated by electrophoresis on 2% agarose gel, which were stained with ethidium bromide (19).

*Measurement of Caspase-3 Activity*—Cells were seeded into 12-well tissue culture plates at a concentration of 4 × 10$^4$ KB cells and treated with TAS-103, bafilomycin A1, and a combination of these drugs for 36 h. The cells were removed by trypsinization and resuspended in hypotonic cell lysis buffer (25 mM HEPES-KOH (pH 7.5), 5 mM MgCl$_2$, 5 mM EDTA, 5 mM DTT, 2 mM PMSF, 10 μg/ml pepstatin A, and 10 μg/ml leupeptin). Following centrifugation for 20 min at 4 °C in a microcentrifuge, the supernatant fractions were collected. The fluorescence (CPP32 activity) of each sample was analyzed with the Fluorometric CaspACE™ Assay System (Promega, Madison, WI) according to the manufacturer's instructions. For caspase activity with CaspACE™ FITC-VAD-FMK *in situ* marker (Promega, Madison, WI), KB cells were treated with TAS-103, bafilomycin A1, and a combination of these drugs for 48 h. Cells were stained with CaspACE™ FITC-VAD-FMK *in situ* marker according to the manufacturer's instructions and analyzed using fluorescence microscopy. For statistical analysis of each experiment, 4 fields (×400) were counted per stimulation and cell type (between 300 and 400 cells in total).

### RESULTS

To isolate genomic clones encoding the 5' region of the *ATP6L* gene, a human genomic library was screened with a previously isolated *ATP6L* cDNA clone (13). Two clones containing non-identical inserts were characterized. The restriction map of these clones is shown in Fig. 1*A*, and sequence analysis confirmed that they encode *ATP6L*. To localize the first exon more accurately, the promoter proximal plasmid was digested with restriction enzymes and analyzed by Southern blotting using cDNA. In order to determine the nucleotide sequence of the promoter region, a 1.9-kb *Eco*RI-*Sal*I fragment of EMBL3 was subcloned into pUC18 (Fig. 1*A*), and the nucleotide sequence of the first exon and its 5'-flanking region were determined (Fig. 1*B*). This fragment contained exons with sequences identical to the 5' portion previously determined from cDNA.

To define precisely the transcription initiation site, we performed primer extension. The cDNA products extended from the primer were analyzed by electrophoresis and sequenced using the same primer. Two major transcription initiation sites were observed (Fig. 2). About 20% of the transcripts initiated at +1 and 80% initiated at +75. The transcription initiation site of the human gene is located 236 bp upstream from that of the mouse gene (29). An additional 100-bp sequence of the 5'-untranslated region has been published. This indicates that the transcription initiation sites of the human gene are completely different from those of the mouse gene. The nucleotide sequences of the factor binding sites are also not the same, suggesting that regulation of the human gene differs from that of the mouse.

Analysis of the region upstream of the first exon failed to locate any sequence motifs such as TATA and CCAAT boxes. There were four GC boxes and one Oct1-binding site in the proximal promoter region, with one GC box on its own in the untranslated region. The GC content around the first exon was about 70%. To determine whether the region upstream of the first exon possesses promoter activity, the available restriction sites were utilized to construct a series of deletion reporter constructs. These constructs were tested by transient transfection in human cancer cell lines KB, PC3, and MCF7 cells. DNA extending only as far as −113 yielded full promoter activity, whereas the region between +57 and +194 retained 50% of maximum activity (data not shown).

We reported previously that V-ATPase gene expression is induced by cisplatin treatment (13) and examined further upregulation of the V-ATPase genes by anticancer agents. As shown in Fig. 3*A*, the steady-state mRNA levels of two V-ATPase genes, *ATP6L* and *-6E*, increased 3–5-fold when cells were treated with cisplatin and TAS-103. To determine whether c and E subunit protein levels also increased when
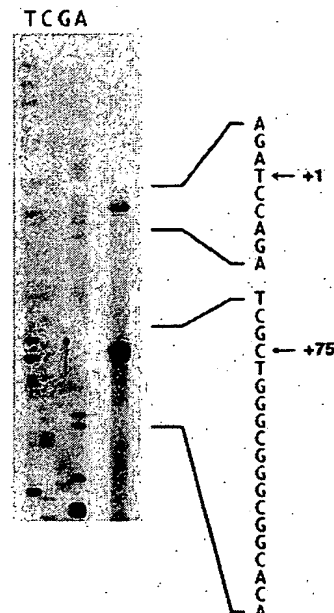
FIG. 1. **Restriction map and sequence of the c subunit promoter.** *A*, restriction endonuclease map of two overlapping *ATP6L* genomic clones. V-ATPase c subunit (*ATP6L*) genomic clones were isolated from a human placental genomic library. Restriction enzyme sites are as follows: *S, Sal*I; *E, Eco*RI; *Bst, Bst*EII; *P, Pst*I; *Bsh, Bsh*TI; and *N, Nar*I. Overlapping regions within these clones were confirmed by Southern blotting. The *Eco*RI–*Sal*I fragment (1.9 kb) contains the first exon and 5′-flanking sequence. *B*, nucleotide sequence of the 5′-upstream region and the first exon of the *ATP6L* gene. Nucleotides are numbered relative to the transcription initiation site, determined by primer extension. The first exon is *boxed*, and the intron sequence is in *lowercase*. The sequences that serve as recognition sites for Sp1 (5′-GGGCGG-3′) and Oct1 (5′-ATGCAAAT-3′) are *underlined* and *double underlined*, respectively. The ATG initiation site is in **boldface**. The *arrow* indicates the position of the primer used for primer extension.



FIG. 2. **Primer extension analysis of the *ATP6L* gene.** The synthetic oligonucleotide 5′-GTCACATGACCTGGGCCCCG-3′ was 5′-end-labeled. The template for reverse transcription was 5 μg of yeast tRNA (*lane 1*) or 5 μg of KB poly(A) RNA (*lane 2*). Electrophoresis was in a 7 M urea, 6% acrylamide DNA sequencing gel.

cells were treated with TAS-103, we performed Western blotting and immunoprecipitation using antibody against the E subunit. As expected, TAS-103 increased the expression of the E subunit (Fig. 3*B*). Immunoprecipitation assay showed that levels of the c (16 kDa), c″ (19 kDa), and D subunits (34 kDa) also increased (Fig. 3*C*). We also analyzed the levels of the higher molecular weight V-ATPase subunits in 10% SDS-PAGE. The levels of subunit a (100–116 kDa), subunit A (70–73 kDa), and subunit C (40–45 kDa) were increased after TAS-103 treatment (Fig. 3*D*). These results indicate that TAS-103 may stimulate the expression of the V-ATPase complex as a whole. Next, we investigated whether the up-regulation of V-ATPase gene expression is because of transcriptional activation, and we found that TAS-103 could activate the promoter of the *ATP6L* and -*6E* genes but cisplatin could not (Fig. 4*A*). On the other hand, cisplatin and TAS-103 both reduced the rate of degradation of *ATP6L* and -*6E* mRNAs (Fig. 4*B*). These find-

ings suggest that drug treatments can promote expression of the V-ATPase by both transcriptional and post-transcriptional mechanisms.

Many potential GC boxes or related motifs are found among the GC-rich stretches in the promoter region. In order to confirm the existence of functional GC boxes and other transcription factor binding sites, we performed an *in vivo* footprint experiment as shown in Fig. 5. Because this experiment was performed using primers for the lower strand, transcription factor bindings to the complementary strand of the nucleotide sequence shown in Fig. 5 were detected. Protection of four 5′-guanines and hypersensitivity of the 3′-guanine of the consensus 5′-GGGCGG-3′, which are typical Sp1 guanine binding signals, were observed at two potential GC box sequences (−73 to −68 and −36 to −31). In addition, there was slight protection of guanines at −84 and −61 on the lower strand surrounding the distal GC box (−73 to −68). Although the proximal GC box (−36 to −31) overlapped with an additional GC box (−41 to −36), a typical profile of Sp1 binding was not detected on this upstream GC box (−41 to −36). No signs of any binding to other tentative GC boxes located downstream of the transcription start site and GC box-like motif (−91 to −86) were seen in experiments with upper strand primers (data not shown).

In order to show that Sp1 (−73 to −68) and Oct1 (−64 to −57) bound specifically to the V-ATPase c promoter *in vivo*, we utilized the chromatin immunoprecipitation assay as shown in Fig. 6. PCR amplification of the V-ATPase c promoter was carried out with DNA extracted from the immunocomplex. Fig. 6*A* shows that significant levels of the V-ATPase c promoter sequence were detected as a 120-bp PCR product in the complexes immunoprecipitated with anti-Sp1 and anti-Oct1 antibody. The *YB-1* promoter sequence was not detected, because there are no Sp1- and Oct1-binding sites in the *YB-1* promoter, as shown in Fig. 6*B*. Furthermore, the V-ATPase c promoter sequence was not observed when normal rabbit IgG was used.
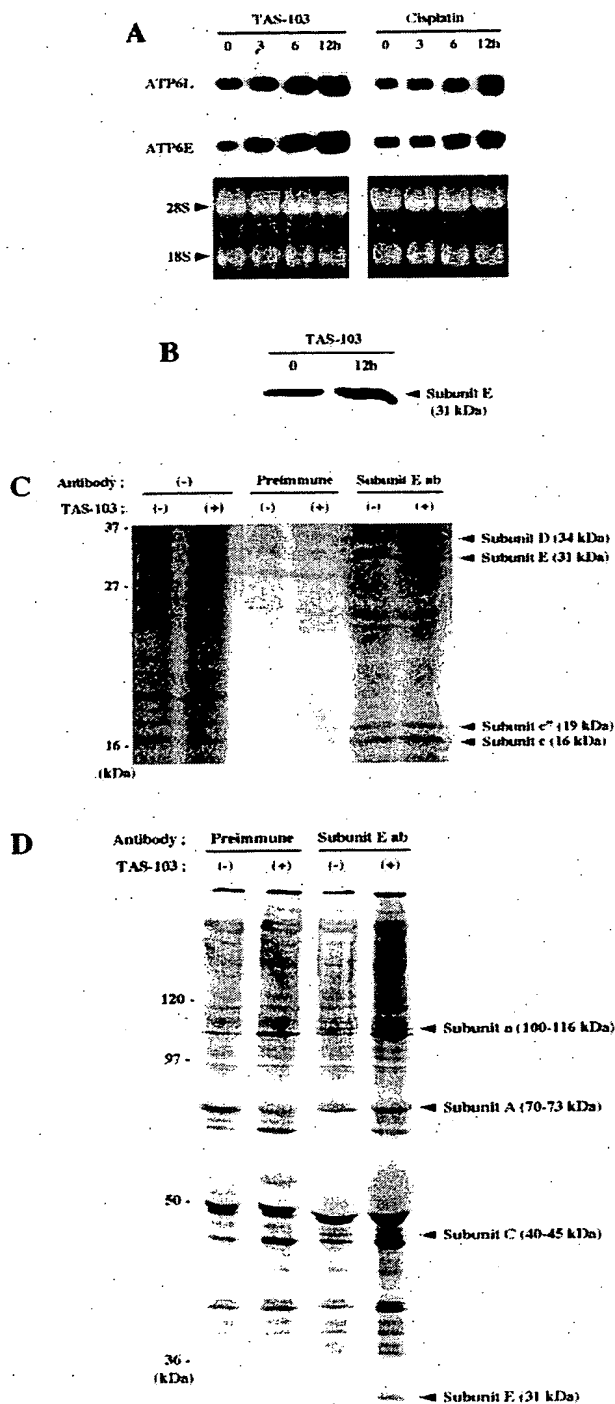
**Fig. 3. Induction of V-ATPase subunits in KB cells treated with anticancer agents.** *A*, effect of anticancer agents on expression of *ATP6L* and *-6E* mRNA. KB cells were incubated with TAS-103 (4 μM) or cisplatin (10 μM) for the times indicated, and the steady-state levels of *ATP6L* and *6E* mRNA were assayed by Northern blotting. 20 μg of total RNA was loaded per lane. *B*, induction of E subunit protein in KB cells treated with TAS-103. KB cells were treated with TAS-103 (4 μM) for 12 h. Cells were harvested and membrane fractions were prepared as described under "Materials and Methods." Forty μg of membrane
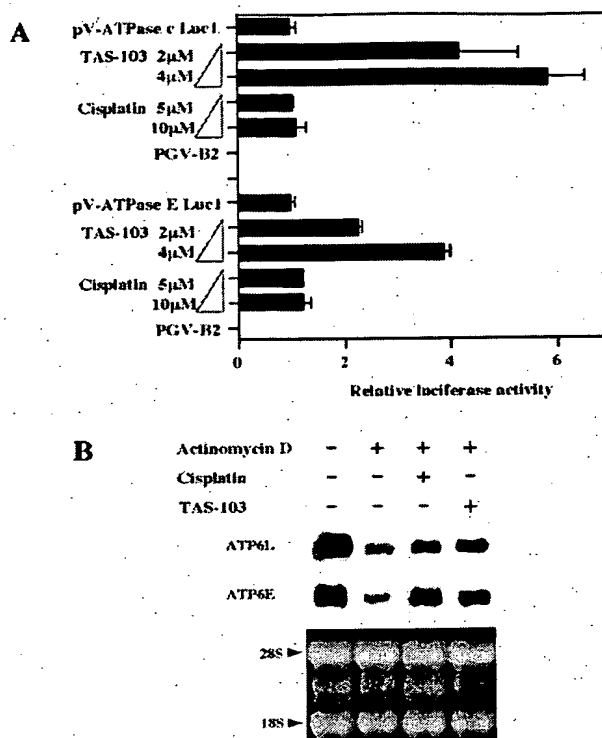


**Fig. 4. Transcriptional activity and mRNA stability of the ATP6L and -6E genes in KB cells treated with anticancer agents.** *A*, transcriptional activity of the *ATP6L* and *-6E* genes in response to anticancer agents. The 5′-flanking regions of the *ATP6L* (nt −1627 to nt +194) and the *-6E* (nt −715 to nt +132) genes were subcloned in basic vector 2 (*B2*) containing a luciferase reporter. The resulting constructs were transiently transfected into KB cells, together with a β-galactosidase reporter as an internal control. After transfection for 12 h, the cells were incubated for 12 h in fresh medium or in medium containing either TAS-103 or cisplatin. Luciferase activity was measured as described under "Materials and Methods." *Error bars* indicate S.D. *B*, stability of *ATP6L* and *-6E* gene transcripts in KB cells treated with anticancer agents. KB cells were incubated with actinomycin D (1 μg/ml) and cisplatin (10 μM) or TAS-103 (4 μM) for 6 h, and the steady-state levels of *ATP6L* and *6E* mRNAs were assayed by Northern blotting. 20 μg of total RNA was loaded per lane.

We next examined the effect of TAS-103 on luciferase activity induced by a series of 5′-deleted promoter constructs assayed 12 h after transfection (Fig. 7*A*). The luciferase activity of Luc1–3 was increased by about 3–6-fold compared with the control by 4 μM TAS-103. The activity of Luc4 was, however, not increased. These results suggest that an element responsible for V-ATPase c promoter activation by TAS-103 is located between −77 and −58. This region contains the GC box and the Oct1-binding site. To examine whether mutations of either the GC box or the Oct1-binding site affect the stimulation of V-

fractions were loaded on a 15% SDS-PAGE gel and transferred to a polyvinylidene difluoride membrane. Immunoblot analysis was performed with antiserum to the V-ATPase E subunit. *C* and *D*, immunoprecipitation with antiserum to the V-ATPase E subunit. Antisera to the V-ATPase E subunit or preimmune binding protein A/G-agarose were incubated for 12 h at 4 °C with [35S]-labeled protein from KB cells with or without exposure to TAS-103 (4 μM). The mixtures were washed three times and separated on a 15% (*C*) or 10% SDS-PAGE gel (*D*). Molecular mass markers are indicated, as well as the positions of proteins that probably correspond to the low molecular weight V-ATPase subunits D and E, c″, c (*C*), and the high molecular weight subunits a, A, C, E (*D*).
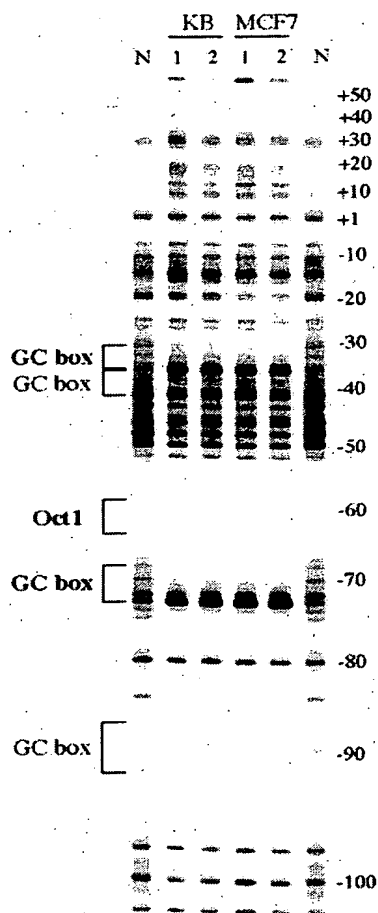
**FIG. 5. In vivo footprint analysis of the *ATP6L* promoter.** The panel shows the lower (transcribed) strand. The potential *cis*-acting DNA element is shown at the *left* of the panel, and the positions relative to the transcription initiation site are shown to the *right*. Lane N contains naked DNA, purified from untreated KB and MCF7 cells and treated with DMS *in vitro*. Lanes *1* and *2* indicate DNA from nuclei treated *in vivo* with 0.05 and 0.1% DMS, respectively. Functional GC boxes and the Oct1-binding site are in *boldface*.

ATPase c promoter activity by TAS-103, we made three constructs with mutations in the promoter sequences of these binding elements (Fig. 7*B*). TAS-103 responsiveness was reduced when a mutation was introduced into the GC box, and mutation of the Oct1-binding sequence completely inhibited TAS-103-induced luciferase activity, suggesting that the Oct1-binding site has a role in the promotion of V-ATPase c expression by TAS-103. The Luc3m1, Luc3m2, and Luc3m3 mutations had no apparent effect on basal transcriptional activity in the absence of TAS-103 (Fig. 7*B*).

To investigate whether V-ATPase c gene transcription activated by TAS-103 was affected by an interplay between Sp1 and Oct1, we performed EMSA on KB cells following TAS-103 treatment to study the interaction between the promoter and transcription factors using nuclear extracts made in buffer S. Six probes were utilized covering the entire core promoter, as described under "Materials and Methods." When Oligos 1, 5, and 6 were used as probes, we could not detect any retarded band (data not shown). However, a retarded band was observed when Oligos 2–4 were used, and its strength was increased by
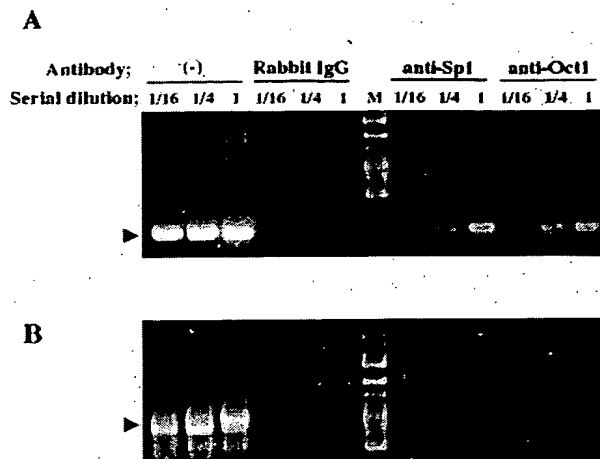


**FIG. 6. Chromatin immunoprecipitation with anti-Sp1 and anti-Oct1 antibody.** Formaldehyde cross-linked chromatin was isolated from KB cells. Chromatin was immunoprecipitated with anti-Sp1, anti-Oct1 antibody, and normal rabbit IgG. Immunoprecipitated DNA was purified and analyzed by PCR using primers specific for either the V-ATPase c promoter (*A*) or the *YB-1* promoter (*B*). The amounts of DNA in the positive controls were 6.25, 25, and 100 ng (*right to left*). Immunoprecipitated DNA was serially diluted to 1, 1/4, and 1/16 (*right to left*). Amplification products were electrophoresed in 2% agarose gel containing ethidium bromide. *M*, DNA ladder mix marker (MBI, Fermentas, Lithuania). *Arrowheads* show 120-bp DNA of the V-ATPase c promoter sequence (*A*) and 725-bp DNA of *YB-1* promoter sequence (*B*).

treatment with TAS-103 (Fig. 8*A*). GC boxes were present in each of these three oligonucleotide probes, and the intensity of the retarded band was reduced by addition of unlabeled GC box DNA (data not shown). Furthermore, the retarded bands were supershifted by antibody to Sp1 but not by antibody to Sp3 or preimmune antibody (Fig. 8*B*).

We noted that the band retarded by Oligo3 probe was not completely shifted by the addition of an excess of Sp1 antibody (data not shown). Oligo3 contains a GC box and an Oct1-binding site. We used nuclear extracts made with two different buffers, as shown under "Materials and Methods," to examine the specificity of the DNA-protein interaction by appropriate competition assays. The band retarded by the nuclear extract prepared in buffer S was also only completely eliminated by a 25-fold excess of unlabeled Oligo3 but not by Oligo3m1, Oligo3m2, and Oligo3m3. On the other hand, the band retarded by the nuclear extract prepared in buffer C was almost completely eliminated by a 25-fold excess of unlabeled Oligo3m1 as well as Oligo3 but not by Oligo3m2 and Oligo3m3 (Fig. 8*C*). These results suggest that only Oct1 binds to the Oligo3 probe when the nuclear extract is prepared in buffer C but that either Sp1 or Oct1 bind to Oligo3 in a mutually exclusive manner when the nuclear extract is prepared in buffer S. We performed supershift assays to confirm these results (Fig. 8*D*). The retarded band was completely shifted by the addition of the Oct1-specific antibody when the nuclear extract was prepared with buffer C, suggesting that only Oct1 can bind to the Oligo3 probe under these conditions. Furthermore, the retarded band was shifted by the addition of either Sp1- or Oct1-specific antibody when the nuclear extract was prepared with buffer S. This indicates that both Sp1 and Oct1 can bind to the Oligo3 but that Sp1 and Oct1 cannot bind simultaneously to the same oligonucleotide. However, the *in vivo* footprint clearly showed that both Sp1 and Oct1 could bind simultaneously *in vivo*.

We next analyzed the DNA-protein complex in more detail after prolonged electrophoresis. Two complexes (C3 and C6)
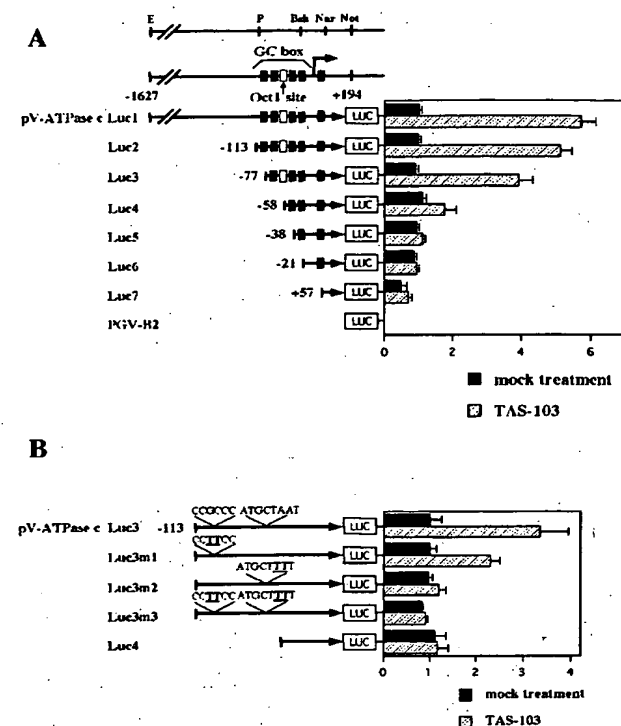
**A**



**B**



FIG. 7. **Functional analysis and deletion mapping of the human *ATP6L* promoter in KB cells.** *A*, schematic representation of the *ATP6L*-luciferase reporters and the relative promoter activity of the *ATP6L* gene. Deletion constructs of the 5'-flanking region of the *ATP6L* gene were subcloned into basic vector 2 upstream of the luciferase reporter gene. All reporter constructs were transiently transfected into KB cells, together with a β-galactosidase reporter as an internal control. After transfection for 12 h, the cells were incubated for 12 h in fresh medium or in medium containing TAS-103 (4 μM). The sequences that serve as the recognition sites for Sp1 are shown as *black boxes*, and those for Oct1 as the *white box. Error bars* indicate S.D. *B*, transcriptional activity of luciferase reporters with mutant Sp1- or Oct1-binding sites. Three constructs with mutations introduced into the Sp1-binding site (Luc3m1), the Oct1-binding site (Luc3m2), and both the Sp1 and Oct1 sites (Luc3m3) were subcloned into basic vector 2 upstream of the luciferase reporter gene. The wild-type sequence of the Sp1 and Oct1 sites is 5'-CCGCCCCGTATGCTAAT-3' (Luc3). The mutant sequences are as follows: 5'-CCTTCCCGTATGCTAAT-3' (Luc3m1), 5'-CCGC-CCCGTATGCTTTT-3' (Luc3m2), and 5'-CCTTCCCGTATGCTTTT-3' (Luc3m3). Luciferase assays were carried out as described.

were formed with Oligo3 (Fig. 9*A*). Both can be supershifted with either anti-Sp1 antibody (C2 and C5) or Oct1 antibody (C1 and C4). This indicates that the slower migrating complex C3 is the complex formed with Sp1 and Oct1 simultaneously, and the faster migrating complex C6 appears to involve either Sp1 or Oct1. Similar results were obtained with the artificial oligonucleotides Oligo3SR and Oligo3–5bp. Both Sp1 and Oct1 binding and promoter activation were slightly enhanced when the phase of the Sp1-binding site was reversed. On the other hand, promoter activity was reduced when 5 bp were inserted between the Sp1- and the Oct1-binding sites (Fig. 9*B*).

Because both Sp1 and Oct1 binding was increased in nuclear extracts prepared from drug-treated cells, we investigated whether these transcription factors participated in the cellular response to TAS-103. As shown in Fig. 10*A*, the cellular levels of both Sp1/Sp3 and Oct1 increased substantially in a time-dependent manner in KB cells exposed to 4 μM TAS-103. To investigate further the role of Sp1 and Oct1 in V-ATPase c promoter activity, the cDNA expression plasmids Sp1, Sp3,

Oct1, and Oct2 were co-transfected into PC3 cells together with the Luc3 plasmid and promoter activity assayed 24 h later (Fig. 10*B*). The results are expressed relative to the activity observed after co-transfection of empty plasmid with the Luc3 reporter. As shown in Fig. 10*B*, co-transfection of the Oct1 expression plasmid increased Luc3 promoter activity ~1.7-fold, whereas co-transfection of the Sp1, Sp3, and Oct2 expression plasmids had no effect. These data suggest that an increase in Oct1 may be critical for the TAS-103-induced up-regulation of V-ATPase c subunit.

In order to better understand the mechanism underlying TAS-103-induced up-regulation of V-ATPase, we tested whether treatment with a V-ATPase inhibitor together with TAS-103 would increase apoptosis. KB cells were treated with a low dose of TAS-103 in the presence or absence of bafilomycin A1 (30, 31), and apoptosis was assessed by DNA fragmentation (Fig. 11*A*), an increase of caspase-3 activity (Fig. 11*B*), and *in situ* labeling of activated caspase (Fig. 11*C*). Apoptosis was significantly stimulated by the combined treatment, suggesting that V-ATPase functions as an anti-apoptotic factor.

## DISCUSSION

We have described the cloning and characterization of the human vacuolar H$^+$-ATPase subunit c (*ATP6L*) gene, and we have isolated overlapping genomic clones encompassing 10 kb of its 5' sequence and 14 kb of its 5'-flanking region (Fig. 1*A*). We determined the nucleotide sequence surrounding the 5' end of the gene that contains the initiation sites for transcription. The regulatory regions are highly GC-rich, and the CpG islands are located 5' to the first exon. Thus, the *ATP6L* promoter has structural features common to housekeeping genes. No typical TATA and CCAAT boxes exist in the region preceding the first exon (Fig. 1*B*), and this may account for the presence of two major transcription initiation sites (Fig. 2). Multiple GC boxes are found in the promoter and first exon. GC boxes are frequent DNA elements present in many promoters and are required for appropriate expression of many ubiquitous genes. This feature of the *ATP6L* 5' region is consistent with its ubiquitous expression in human tissues and suggests that it encodes a protein with an essential cellular function.

Recently, the nucleotide sequence of the mouse V-ATPase c subunit promoter has been reported (29). Although there is significant homology between the proximal promoter sequence of human and mouse, the GC boxes are not conserved in the mouse gene. Furthermore, it is noteworthy that the human transcription initiation site is completely different from that of the mouse. The human *ATP6L* cDNA sequence has been published, and based on a sequence alignment of human cDNA, human cDNA has an additional 100 bp compared with the mouse initiation site. This indicates that the human and the mouse *ATP6L* genes are differently regulated.

As shown in Fig. 3*A*, mRNA levels of two V-ATPase genes were significantly (3–5-fold) up-regulated when cells were treated with TAS-103. Quantitation by PhosphorImager indicates that the protein levels of V-ATPase subunits c and E increased only 1.5–2-fold compared with a dramatic increase of mRNA. This discrepancy is probably due to the translational or post-translational control of V-ATPase protein. Functional analysis of the promoter region in a transient expression system demonstrated significant promoter activity in human cancer cells, and this activity increased 3–6-fold in TAS-103-treated cells (Fig. 4*A*). Furthermore, the region between −77 and −58 was required for the transcriptional up-regulation (Fig. 7*A*). Protein DNA interaction on the proximal promoter region was investigated by *in vivo* DMS footprint experiments. We detected clear evidence of Sp1 binding to two GC boxes. As
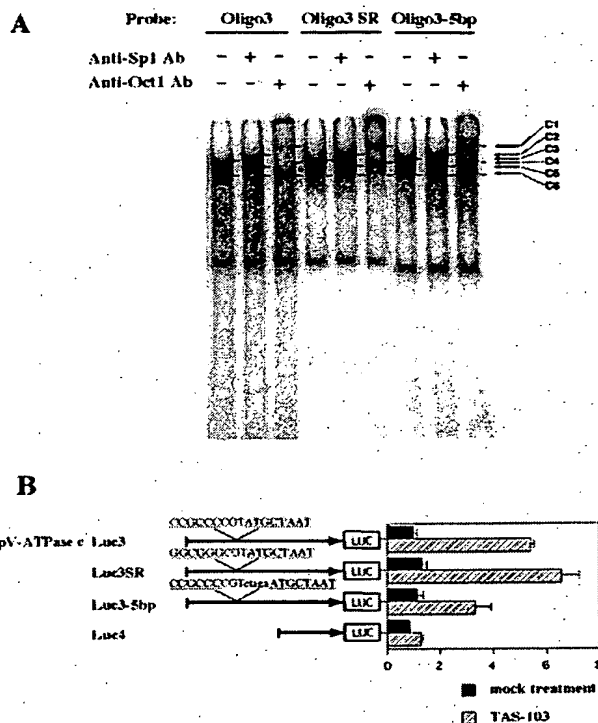
**A**

Probe: Oligo2 Oligo3 Oligo4
TAS-103  0  12h  0  12h  0  12h

◄ F

**B**

Probe:  Oligo2  Oligo3  Oligo4

Anti-Sp1 Ab  − + − −  − + − −  − + − −
Anti-Sp3 Ab  − − + −  − − + −  − − + −
Mouse IgG  − − − +  − − − +  − − − +

◄ F

**C**

Competitor
Oligo 3 | Oligo3m1 | Oligo3m2 | Oligo3m3

Competitor
Oligo 3 | Oligo3m1 | Oligo3m2 | Oligo3m3

◄F

Buffer C                    Buffer S

**D**

Buffer C          Buffer S

◄F

Probe: Oligo3

FIG. 8. **Characterization of proteins binding to regions of the human *ATP6L* promoter.** *A*, EMSA with the six core promoter oligonucleotides. Nuclear extracts from TAS-103 (4 μM) treated for 12 h and untreated KB cells, made using buffer S, were reacted with each of the
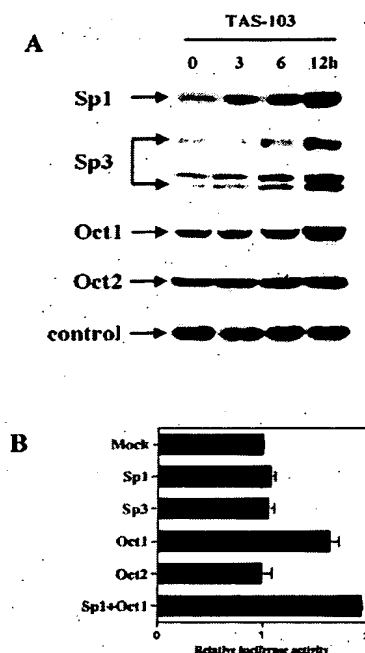
**A**

Probe:  Oligo3  Oligo3 SR  Oligo3-5bp

Anti-Sp1 Ab  − + −  − + −  − + −
Anti-Oct1 Ab  − − +  − − +  − − +

C1
C2
C3
C4
C5
C6

**B**

pV-ATPase c Luc3

Luc3SR

Luc3-5bp

Luc4

0    2    4    6    8

■ mock treatment
▨ TAS-103

FIG. 9. **Cooperation between Sp1 and Oct1 at the *ATP6L* promoter.** *A*, EMSA with mutant forms of Oligo3. Labeled oligonucleotides with reversed GC box (*Oligo3SR*) or a 5-bp sequence inserted between the Sp1 and Oct1 sites (*Oligo3–5bp*) were prepared as described under "Materials and Methods." Buffer S nuclear extracts of KB cells treated with TAS-103 (4 μM) were incubated with probes and 2 μg of anti-Sp1 or anti-Oct1 antibody (*Ab*) for 30 min at 4 °C. The slower migrating band (*C3*) is a complex formed with both Sp1 and Oct1, the faster migrating band (*C6*) is formed with either Sp1 or Oct1. *C1–6* refer to the following: *C1*, Sp1 + Oct1 + anti-Oct1 antibody; *C2*, Sp1 + Oct1 + anti-Sp1 antibody; *C3*, Sp1 + Oct1; *C4*, Oct1 + anti-Oct1 antibody; *C5*, Sp1 + anti-Sp1 antibody; *C6*, Sp1 or Oct1. *B*, luciferase assay with the mutant reporter plasmids. Reporter plasmids with reversed GC box (*Luc3SR*), or a 5-bp insertion between the Sp1- and Oct1-binding site (*Luc3-5bp*), were constructed. The mutated sequences are 5'-GGCGGGCGTATGCTAAT-3' (*Luc3SR*) and 5'-CCGCCCCGTctagaAT-GCTTTT-3' (*Luc3–5bp*). Luciferase assay was carried out as described under "Materials and Methods."

shown in Fig. 5, the G residue in the octamer sequence was protected in the footprint. Also, the V-ATPase c promoter sequence that contains both Sp1- and Oct1-binding sites was recovered in complexes immunoprecipitated with either anti-

oligonucleotides as described under "Materials and Methods." The *arrow* indicates the principal retarded band, and *F* denotes free probe. *B*, analysis of GC box-binding proteins by supershift assay. Nuclear extracts from TAS-103 (4 μM)-treated KB cells, made using buffer S, were incubated with probes and 2 μl of anti-Sp1 or anti-Sp3 antibody (*Ab*) for 30 min at 4 °C. The position of the supershifted band is indicated by the *arrow*. *F* indicates the free probe. *C*, ability of mutated oligonucleotides to compete for Oligo3 binding. Oligonucleotides with mutations in the GC box (Oligo3m1), in the Oct1-binding site (Oligo3m2), and in both sites (Oligo3m3) of Oligo3 were prepared as described under "Materials and Methods." 5-, 10-, and 25-fold molar excesses of unlabeled oligonucleotide were preincubated with buffer C or buffer S nuclear extracts from KB cells with or without TAS-103 (4 μM) treatment, and labeled Oligo3 was then added. *F*, free probes. *D*, analysis of GC box and specific octamer sequence binding proteins by supershift assay. Nuclear extracts of KB cells treated with TAS-103 (4 μM), made using buffer C or buffer S, were incubated with probe and 2 μg of anti-Sp1, anti-Sp3, anti-Oct1, or anti-Oct2 antibody for 30 min at 4 °C. The positions of the supershifted bands are indicated by the *arrows*. *F* is the free probe.

A

TAS-103

0    3    6    12h

Sp1 →

Sp3 [

Oct1 →

Oct2 →

control →

B

Mock

Sp1

Sp3

Oct1

Oct2

Sp1+Oct1

0                    1                    2

Relative luciferase activity

Fig. 10. **Western blotting of transcription factors and lucifer-ase assay following co-transfection.** *A,* induction of Sp1, Sp3, Oct1, and Oct2 proteins in KB cells treated with TAS-103. KB cells were treated with TAS-103 (4 $\mu$M). The cells were harvested at 3, 6, and 12 h after treatment, and nuclear extracts were prepared. 100 $\mu$g of nuclear extracts were loaded on a 10% SDS-PAGE gel and transferred to a polyvinylidene difluoride membrane. Immunoblot analysis was performed with an appropriate dilution of anti-Sp1, anti-Sp3, anti-Oct1, or anti-Oct2 antibodies. *Control* indicates Coomassie Brilliant Blue-stained protein. *B,* luciferase assay with expression plasmids. Luciferase reporter plasmids (pV-ATPase c Luc3) were transiently transfected into KB cells, together with expression plasmids for Sp1, Sp3, Oct1, and Oct2. After transfection for 12 h, the cells were incubated for 24 h in fresh medium at 37 °C. Luciferase activity was measured as described under "Materials and Methods." *Error bars* indicate S.D.

Sp1 or anti-Oct1 antibodies in chromatin immunoprecipitation assays (Fig. 6).

In EMSA, specific promoter-DNA binding was stimulated when the cells were treated with TAS-103. When Oligo3 was used as probe, the transcription factors in the protein-DNA complexes were identified as Sp1 and Oct1. Another noteworthy observation was that Sp1 binding was observed in nuclear extracts prepared with buffer S but not with buffer C. Evidently, differences in the way the nuclear extract is prepared can significantly affect the profile of DNA-protein interaction when binding sites for two factors exist in the same probe (Fig. 8, *C* and *D*). Further study is necessary to determine the exact difference between the nuclear extracts prepared with the two different buffers.

Oct1, a member of the POU homeodomain family, is ubiquitously expressed and plays a role in activating transcription of various genes (32, 33). Functional cooperation between Sp1 and Oct1 has been reported in the regulation of the human U2 small nuclear RNA promoter (34). Furthermore, the two transcription factors interact *in vivo* in the yeast two-hybrid system and regulate human U2 small nuclear RNA genes (35), indicating that both transcription factors are necessary for basal transcriptional activity of this gene. Recently, Oct1 has been shown to be induced after cells are treated with DNA-damaging agents and anticancer agents, including UV irradiation, cisplatin, etoposide, and camptothecin (36, 37). We have confirmed
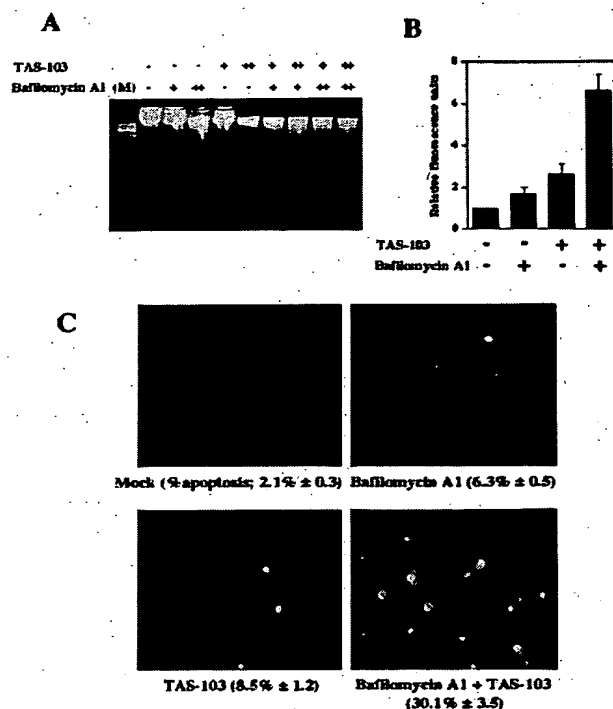
A

TAS-103     · · · · + ++ + ++ + ++
Bafilomycin A1 (M) · + ++ · · + + ++ ++

B

TAS-103     ·   ·   +   +
Bafilomycin A1 ·   +   ·   +

C

Mock (% apoptosis; 2.1% ± 0.3)     Bafilomycin A1 (6.3% ± 0.5)

TAS-103 (8.5% ± 1.2)     Bafilomycin A1 + TAS-103 (30.1% ± 3.5)

Fig. 11. **DNA fragmentation and caspase-3 activity.** *A,* DNA fragmentation in KB cells treated with anticancer agents. KB cells were treated with TAS-103, bafilomycin A1, and a combination of these drugs for 36 h. The cells were harvested and DNA-purified. DNA samples were separated by electrophoresis on 2% agarose gels and stained with ethidium bromide. TAS-103 + and ++ indicates 0.2 and 0.5 $\mu$M, and bafilomycin A1 + and ++ indicates 2 and 5 nM. *M* indicates DNA ladder mix marker. *B,* caspase-3 (CPP32) activity in KB cells treated with anticancer agents. KB cells were treated with TAS-103 (0.2 $\mu$M), bafilomycin A1 (5 nM), or both for 36 h. Fluorescence was measured with the CaspACE™ Assay System according to the manufacturer's instructions. *Error bars* indicate S.D. *C, in situ* detection of activated caspase in KB cells treated with anticancer agents. KB cells were treated with TAS-103 (0.1 $\mu$M), bafilomycin A1 (5 nM), or both for 48 h. The cells were then stained with CaspACE™ FITC-VAD-FMK *in situ* marker according to the manufacturer's instructions. Four fields (×400) were counted per stimulation and per cell type (between 300 and 400 cells in total).

that both camptothecin and etoposide induce *ATP6L* promoter activity (data not shown). However, we could not detect promoter activation when cells were treated with cisplatin (Fig. 4A). To our knowledge, the present study is the first to demonstrate activation of Oct1 target genes after treatment with anticancer agents.

V-ATPase subunit genes are inducible by treatment of human cancer cells with cisplatin and are up-regulated in cisplatin-resistant cell lines (13). Transient transfection of a reporter plasmid showed that promoter activity is not activated by cisplatin treatment (Fig. 4A) and is not enhanced in resistant cell lines (data not shown). One possible explanation is that post-transcriptional mechanisms, such as mRNA stabilization, may be involved in the cisplatin induction and up-regulation of this gene in drug-resistant cells. Another possibility is that the pathway signaling DNA damage to transcription factors may differ between cisplatin and other anticancer agents. Because cisplatin can block degradation of the mRNA (Fig. 4B), certain pathways signaling DNA damage in human cancer cells may increase mRNA stability.

Our data indicate that drug-induced gene expression is regulated by both transcriptional and post-transcriptional mech-

anisms. We have demonstrated induction of Sp1/Sp3 and Oct1 in response to anticancer agents (Fig. 10*A*). In contrast to the untreated cells, induction of both Sp1 and Sp3 protein was observed to increase 5–10-fold. The level of Oct1 protein was observed to increase 3–5-fold. Sp3 might act as repressor to inhibit Sp1-dependent transcription, suggesting that Sp1-dependent transcription of *ATP6L* gene is reduced by the Sp3 induced by TAS-103. Thus, induction of *ATP6L* mRNA might be substantially affected by the induction of Oct1. The results of both Northern blot analysis and reporter assays were consistent with those of the Oct1 induction. Both co-transfection experiments and reporter assays with mutated promoters confirm that Oct1 is the main factor involved in the induction of promoter activity by TAS-103. Because both Sp1 and Oct1 are ubiquitously expressed, these housekeeping transcription factors may cooperate with other transcription factors, including basal transcription factors and cofactors, to protect cells from genotoxic stress. We have shown that Sp1 binds to the two GC boxes located in the proximal promoter region of *ATP6L*. Sp1 is not the only a protein acting through GC boxes; the existence of a small protein family consisting of Sp1, Sp2, Sp3, and Sp4 has been reported (38–41). Hence the absolute levels of Sp1 and Sp3 or their nuclear ratio may be responsible for differences in promoter binding and target genes expression. The transcriptional cofactors required for Sp1 activity have been identified (42), further emphasizing that these cofactors may be involved in the activation of Sp1 target genes in response to anticancer agents. The exact mechanisms by which Sp1 and Oct1 act on the expression of target genes to promote tumorigenesis and drug resistance remain unclear.

Expression of V-ATPase could have significance for cell growth (43), cell motility (44), tumorigenesis (45), metastasis (46), and apoptosis (47). The reason for induction of V-ATPase by anticancer agents is unclear, but increased V-ATPase activity may represent a cellular anti-apoptotic response. Our results show that TAS-103 can induce apoptosis, especially in the presence of bafilomycin A1 (Fig. 11), suggesting that V-ATPase inhibits apoptosis of cancer cells by preventing cellular acidosis. It will be of considerable interest to identify the transcription factors that regulate the expression of other V-ATPase subunit genes, and studies along these lines are in progress.

## REFERENCES

1. Stevens, T. H., and Forgac, M. (1997) *Annu. Rev. Cell Dev. Biol.* 13, 779–808
2. Finbow, M. E., and Harrison, M. A. (1997) *Biochem. J.* 324, 697–712
3. Forgac, M. (1998) *FEBS Lett.* 440, 258–263
4. Forgac, M. (1999) *J. Biol. Chem.* 274, 12951–12954
5. Nishi, T., and Forgac M. (2002) *Nat. Rev. Mol. Cell Biol.* 3, 94–103
6. Torigoe, T., Izumi, H., Ise, T., Murakami, T., Uramoto, H., Ishiguchi, H., Yoshida, Y., Tanabe, M., Nomoto, M., and Kohno, K. (2002) *Anti-Cancer Drugs* 13, 237–243
7. Wieczorek, H., Brown, D., Grinstein, S., Ehrenfeld, J., and Harvey, W. R. (1999) *Bioessays* 21, 637–648
8. Merzendorfer, H., Graf, R., Huss, M., Harvey, W. R., and Wieczorek, H. (1997) *J. Exp. Biol.* 200, 225–235
9. Wieczorek, H., Gruber, G., Harvey, W. R., Huss, M., Merzendorfer, H., and

Zeiske, W. (2000) *J. Exp. Biol.* 203, 127–135
10. Bowman, B. S., Dschida, W. J., Harris, T., and Bowman, E. J. (1989) *J. Biol. Chem.* 264, 15606–15612
11. Martinez-Zaguilan, R., Lynch, R. M., Martinez, G. M., and Gillies, R. J. (1993) *Am. J. Physiol.* 265, C1015–C1029
12. Laurencot, C. M., Andrews, P. A., and Kennedy, K. A. (1995) *Oncol. Res.* 7, 363–369
13. Murakami, T., Sibuya, I., Ise, T., Zhe-Sheng, C., Akiyama, S., Nakagawa, M., Izumi, H., Nakamura, T., Matsuo, K., Yamada, Y., and Kohno, K. (2001) *Int. J. Cancer* 93, 869–874
14. Martinez-Zaguilan, R., Raghunand, N., Lynch, R. M., Bellamy, W., Martinez, G. M., Rojas, B., Smith, D., Dalton, W. S., and Gillies, R. J. (1999) *Biochem. Pharmacol.* 57, 1037–1046
15. Skinner, M. A., and Wildeman, A. G. (1999) *J. Biol. Chem.* 274, 23119–23127
16. Skinner, M. A., and Wildeman, A. G. (2001) *J. Biol. Chem.* 276, 48451–48457
17. Azuma, R., and Urakawa, A. (1997) *J. Chromatogr. B. Biomed. Appl.* 691, 179–185
18. Byl, J. A., Fortune, J. M., Burden, D. A., Nitiss, J. L., Utsugi, T., Yamada, Y., and Osheroff, N. (1999) *Biochemistry* 38, 15573–15579
19. Kluza, J., Lansiaux, A., Wattez, N., Mahieu, C., Osheroff, N., and Bailly, C. (2000) *Cancer Res.* 60, 4077–4084
20. Shen, D. W., Akiyama, S., Schoenlein, P., Pastan, I., and Gottesman, M. M. (1995) *Br. J. Cancer* 71, 676–683
21. Nakagawa, M., Nomura, Y., Kohno, K., Ono, M., Mizoguchi, H., Ogata, J., and Kuwano, M. (1993) *J. Urol.* 150, 1970–1973
22. Furuya, Y., Yamamoto, K., Kohno, N., Ku, Y., and Saitoh, Y. (1994) *Cancer Lett.* 81, 95–98
23. Miura, K., Miyazaki, S., Furuta, S., Mitsushita, J., Kamijo, K., Ishida, H., Miki, T., Suzukawa, K., Resau, J., Copeland, T. D., and Kamata, T. (2001) *J. Biol. Chem.* 276, 46276–46283
24. Koike, K., Abe, T., Hisano, T., Kubo, T., Wada, M., Kohno, K., and Kuwano, M. (1996) *Jpn. J. Cancer Res.* 87, 765–772
25. Konishi, T., Nomoto, M., Shimizu, K., Abe, T., Itoh, H., Friedrich, H., Gunther, E., and Higashi, K. (1995) *J. Biochem. (Tokyo)* 118, 1021–1029
26. Nomoto, M., Gonzalez, F. J., Mita, T., Inoue, N., and Kawamura, M. (1995) *Biochim. Biophys. Acta* 1264, 35–39
27. Rundlof, A. K., Carlsten, M., and Arner, E. S. (2001) *J. Biol. Chem.* 276, 30542–30551
28. Ise, T., Nagatani, G., Imanura, T., Kato, K., Takano, H., Nomoto, M., Izumi, H., Ohmori, H., Okamoto, T., Ohga, T., Uchiumi, T., Kuwano, M., and Kohno, K. (1999) *Cancer Res.* 59, 342–346
29. Wang, S. P., Krits, I., Bai, S., and Lee, B. S. (2002) *J. Biol. Chem.* 277, 8827–8834
30. Bowman, E. J., Siebers, A., and Altendorf, K. (1998) *Proc. Natl. Acad. Sci. U. S. A.* 85, 7972–7976
31. Bowman, B. J., and Bowman, E. J. (2002) *J. Biol. Chem.* 277, 3965–3972
32. Phillips, K., and Luisi, B. (2000) *J. Mol. Biol.* 302, 1023–1039 *
33. Malone, C. S., Patrone, L., Buchanan, K. L., Webb, C. F., and Wall, R. (2000) *J. Immunol.* 164, 2550–2556
34. Janson, L., and Pettersson, U. (1990) *Proc. Natl. Acad. Sci. U. S. A.* 87, 4732–4736
35. Strom, A. C., Forsberg, M., Lillhager, P., and Westin, G. (1996) *Nucleic Acids Res.* 24, 1981–1986
36. Meighan-Mantha, R. L., Riegel, A. T., Suy, S., Harris, V., Wang, F. L., Lozano, C., Whiteside, T. L., and Kasid, U. (1999) *Mol. Cell. Biochem.* 199, 209–215
37. Zhao, H., Jin, S., Fan, F., Tong, T., and Zhao, Q. (2000) *Cancer Res.* 60, 6276–6280
38. Dynan, W. S., and Tjian, R. (1983) *Cell* 35, 79–87
39. Hagen, G., Muller, S., Beato, M., and Suske, G. (1994) *EMBO J.* 13, 3843–3851
40. Hagen, G., Dennig, J., Preiss, A., Beato, M., and Suske, G. (1995) *J. Biol. Chem.* 270, 24989–24994
41. Suske, G. (1999) *Gene (Amst.)* 238, 291–300
42. Ryu, S., Zhou, S., Ladurner, A. G., and Tjian, R. (1999) *Nature* 397, 446–450
43. Helmlinger, G., Yuan, F., Dellian, M., and Jain, R. K. (1997) *Nat. Med.* 3, 177–182
44. Martinez-Zaguilan, R., Martinez, G. M., Gomez, A., Hendrix, M. J., and Gillies, R. J. (1998) *J. Cell. Physiol.* 176, 196–205
45. Perona, R., and Serrano, R. (1998) *Nature* 334, 438–440
46. Schlappack, O. K., Zimmermann, A., and Hill, R. P. (1991) *Br. J. Cancer* 64, 663–670
47. Gottlieb, R. A., Giesing, H. A., Zhu, J. Y., Engler, R. L., and Babior, B. M. (1995) *Proc. Natl. Acad. Sci. U. S. A.* 92, 5965–5968

# Inhibitors of vacuolar H+-ATPase impair the preferential accumulation of daunomycin in lysosomes and reverse the resistance to anthracyclines in drug-resistant renal epithelial cells

Zahia OUAR*, Marcelle BENS*, Caroline VIGNES†, Marc PAULAIS‡, Claudine PRINGEL§, Jocelyne FLEURY§, Françoise CLUZEAUD*, Roger LACAVE§ and Alain VANDEWALLE*[1]

*INSERM U478, Faculté de Médecine Xavier Bichat, 16 rue Henri Huchard, BP 416, 75870 Paris Cedex 18, France, †IFR 02, Faculté de Médecine Xavier Bichat, 16 rue Henri Huchard, BP 416, 75870 Paris Cedex 18, France, ‡INSERM U426, Faculté de Médecine Xavier Bichat, 16 rue Henri Huchard, BP 416, 75870 Paris Cedex 18, France, and §Laboratoire d'Histologie et Biologie Tumorale, Hôpital Tenon, 75020 Paris, France

It has been suggested that the inappropriate sequestration of weak-base chemotherapeutic drugs in acidic vesicles by multidrug-resistance (MDR) cells contributes to the mechanisms of drug resistance. The function of the acidic lysosomes can be altered in MDR cells, and so we investigated the effects of lysosomotropic agents on the secretion of lysosomal enzymes and on the intracellular distribution of the weak-base anthracycline daunomycin in drug-resistant renal proximal tubule PKSV-PR$_{col50}$ cells and their drug-sensitive PKSV-PR cell counterparts. Imaging studies using pH-dependent lysosomotropic dyes revealed that drug-sensitive and drug-resistant cells exhibited a similar acidic lysosomal pH (around 5.6–5.7), but that PKSV-PR$_{col50}$ cells contained more acidic lysosomes and secreted more of the lysosomal enzymes N-acetyl-β-hexosaminidase and β-glucuronidase than their parent PKSV-PR cells. Concanamycin A (CCM A), a potent inhibitor of the vacuolar H+-ATPase, but not the P-glycoprotein modulator verapamil, stimulated the secretion of N-acetyl-β-hexosaminidase in both drug-sensitive and drug-resistant cells. Fluorescent studies and Percoll density gradient fractionation studies revealed that daunomycin accumulated predominantly in the lysosomes of PKSV-PR$_{col50}$ cells, whereas in PKSV-PR cells the drug was distributed evenly throughout the nucleo-cytoplasmic compartments. CCM A did not impair the cellular efflux of daunomycin, but induced the rapid nucleo-cytoplasmic redistribution of the drug in PKSV-PR$_{col50}$ cells. In addition, CCM A and bafilomycin A1 almost completely restored the sensitivity of these drug-resistant cells to daunomycin, doxorubicin and epirubicin. These findings indicate that lysosomotropic agents that impair the acidic-pH-dependent accumulation of weak-base chemotherapeutic drugs may reverse anthracycline resistance in MDR cells with an expanded acidic lysosomal compartment.

Key words: anthracycline, lysosome, multidrug resistance, proton pump, renal cells.

## INTRODUCTION

The multidrug-resistance (MDR) phenomenon that occurs in cancer cells is characterized by the development of resistance to a wide range of structurally and functionally diverse drugs, and it constitutes a major obstacle to chemotherapy. The mechanisms underlying MDR have been studied extensively in models of cultured drug-sensitive and -resistant tumour cells. The change most often observed in MDR cells is increased expression of the P-glycoprotein (P-gp) encoded by the MDR gene, belonging to the superfamily of ATP binding cassette transporters (ABC transporters) [1,2], which causes a decrease in the accumulation of a variety of cytotoxic drugs [1–3]. However, it has been suggested that mechanisms in addition to the extrusion of drugs via ATP-dependent membranous ABC transporters, which result from biophysical changes in either transmembrane pH gradients or electrical potentials, may also play a role in decreasing the accumulation of chemotherapeutic drugs in several cultured MDR cell models [3–5].

The MDR phenomenon can be associated with the over-expression of many other ABC transporters, such as the MDR-associated protein (MRP) and the lung resistant-related protein, and with many changes in the expression of a variety of cytoplasmic and plasma membrane proteins, such as DNA topoisomerase II, vacuolar H+-ATPase, glutathione S-transferase π and catalase (for review, see [3]). As a consequence, the intracellular concentration and distribution of drugs may differ considerably in drug-sensitive and drug-resistant cells. Chemotherapeutic drugs such as the anthracyclines are distributed mainly in the cytoplasm and nucleus of drug-sensitive cells, but can accumulate preferentially in the acidic organelles of a variety of drug-resistant cancer cells [6–11]. Schindler et al. [12] have proposed a 'protonation, sequestration and secretion (PSS)' model that could account for the relative sensitivity of tumour cells to anthracyclines. These authors have reported that adriamycin is concentrated in acidified organelles (i.e. lysosomes and recycling endosomes) from drug-resistant MCF-7/ADR breast cancer cells, but not in those from their drug-sensitive MCF-7 counterparts exhibiting a vesicular acidification defect [11]. These authors and others have also shown that disruption of the pH gradient between the cytoplasm and the acidic organelles by a variety of lysosomotropic agents leads to the release of chemotherapeutic drugs accumulated in the acidic organelles from drug-resistant cells [10,11]. This intravesicular relocation of anthracyclines can obviously be expected to impair their cytotoxic action, which involves nuclear effects, including binding of DNA

and interference with topoisomerase II [13]. However, the contribution of the inappropriate sequestration of drugs in acidic organelles to the MDR phenomenon is still debated [14]. Disruption of the pH gradient between the cytoplasm and the acidic organelles by a variety of lysosomotropic agents may lead to the release of chemotherapeutic drugs accumulated in the acidic organelles from MDR cells; however, its impact on resistance to weak-base chemotherapeutic drugs has not been fully evaluated.

In the kidney, P-gp is expressed in the apical brush border of intact proximal tubule cells [15], which possess an active secretory lysosomal machinery [16]. Most forms of renal adenocarcinoma, which are mainly of proximal tubule origin, are highly resistant to chemotherapy. We established a line of drug-sensitive PKSV-PR cells derived from L-PK/Tag 1 transgenic mice harbouring the pyruvate kinase (PK)-Tag transgene [17], which have maintained the main features of the parent cells from which they were derived [18]. Drug-resistant MDR mouse proximal tubule cells (PKSV-PR$_{col50}$) were then obtained by continuous selection of parent PKSV-PR cells with colchicine [19]. These drug-sensitive and drug-resistant proximal tubule cells therefore appeared to be suitable cell models for an analysis of lysosomal functions and the intracellular distribution of daunomycin. We also used these cells to investigate the consequences of the rapid alkalinization of lysosomes induced by inhibitors of vacuolar H$^{+}$-ATPase for the cellular redistribution of anthracyclines and the restoration of drug sensitivity to drug-resistant proximal tubule cells.

## MATERIALS AND METHODS

### Cell culture

We used PKSV-PR$_{col50}$ cells, a mouse kidney proximal tubule drug-resistant cell line, selected by colchicine from the parent drug-sensitive PKSV-PR cells [19]. PKSV-PR cells were cultured routinely in a modified culture medium [Dulbecco's modified Eagle's medium/Ham's F12, 1:1 (v/v), 60 nM sodium selenite, 5 μg/ml transferrin, 2 mM glutamine, 5 μg/ml insulin, 50 nM dexamethasone, 5 nM tri-iodothyronine, 10 ng/ml epidermal growth factor, 20 mM D-glucose, 2% (v/v) fetal calf serum, 20 mM Hepes, pH 7.4] at 37 °C in a 5% CO$_2$/95% air atmosphere. PKSV-PR$_{col50}$ cells were grown in the same medium supplemented with 50 ng/ml colchicine. All experiments were performed between the 45th and 65th passages, and media were changed every 2 days.

### Daunomycin efflux studies

The rate of efflux of daunomycin was determined as described previously [19] from confluent PKSV-PR and PKSV-PR$_{col50}$ cells grown on collagen-coated six-well plates incubated with 100 nM [G-$^3$H]daunomycin (specific radioactivity 5 Ci/mmol; NEN Life Science Products, Paris, France) for 60 min at 37 °C (loading period). The cell layers were then rinsed with ice-cold serum-free medium and incubated with 2.5 ml of fresh, serum-free, CO$_2$-free medium pre-warmed to 37 °C. Samples of 50 μl were collected at various intervals from 5 to 180 min, cells were lysed in 1 M NaOH and radioactivity was counted.

### Enzyme assays

The activities of lysosomal enzymes were measured in the medium and in confluent cells grown on six-well plates. The culture medium was removed and cells were rinsed with PBS, scraped off, centrifuged (100 g, 5 min) at 4 °C, and stored at −70 °C.

Pelleted cells were resuspended in 1 ml of 10 mM phosphate buffer, pH 7, sonicated and then incubated with 0.1% (v/v) Triton X-100 for 2 h at 4 °C. The N-acetyl-β-hexosaminidase (NAG) activity of the cell lysates and culture medium was measured as described in [16]. Aliquots of cell lysate and medium were incubated in 0.2 ml of 50 mM citric acid/sodium citrate, pH 4.6, 2.5 mM 4-methylumbelliferyl β-N-acetylglucosaminide (Sigma) and 0.2 mg/ml BSA (Miles) for 10 min (lysate) or 30 min (medium) at 37 °C. The reaction was stopped by adding 2.85 ml of 400 mM glycine/NaOH, pH 10.8. The activities of β-glucuronidase and acid phosphatase (AcP) were determined as described above, using 2.5 mM 4-methylumbelliferyl β-glucuronide in 0.1 M sodium acetate/acetic acid buffer, pH 4.5, as the substrate for β-glucuronidase activity, and 1 mM 4-methylumbelliferyl phosphate in 0.1 M sodium acetate/acetic acid buffer, pH 5, as the substrate for AcP activity. The fluorescence intensity of the 4-methylumbelliferone released was measured by fluorimetry (excitation 368 nm, emission 448 nm), using 2.25 mM quinine sulphate solution to calibrate the fluorescence intensity. All measurements were performed in triplicate. The percentage of NAG, β-glucuronidase or AcP secreted into the culture medium was calculated from the ratio of enzymic activity in the culture medium over total activity (medium plus cell lysate).

### Flow cytometry

The nuclear accumulation of daunomycin was assessed by cytofluorimetry. Briefly, cells were incubated sequentially with or without 20 nM concanamycin A (CCM A) for 24 h and with 50 μM daunomycin for 2 h at 37 °C. After rinsing, the cells were resuspended in a lysis buffer containing 0.3% Nonidet P40 and incubated for 5 min at 4 °C as described in [10]. Pelleted nuclei resuspended in 400 μl of PBS were fixed using IntraPrep™ fixation and permeabilization reagents (Immunotech, Marseilles, France). The fluorescence intensity of daunomycin accumulated in the nuclei was measured using a flow cytometer (Elite; Beckman-Coulter), assuming that the fluorescence emission recorded at 625 nm was proportional to the amount of daunomycin incorporated into DNA after its translation into the nuclei.

### Cell imaging studies

Cells were seeded and grown to confluency on Lab-Tek coverglass chambers (Nalge Nunc International, Naperville, IL, U.S.A.). They were incubated in Phenol Red/fetal calf serum-free Dulbecco's modified Eagle's medium containing 20 mM Hepes, pH 7.4, at 37 °C under a flux of a humidified 5% CO$_2$/95% air atmosphere. Imaging was conducted on living cells using a confocal laser scanning inverted microscope (TCS 4D; Leica, Heidelberg, Germany) equipped with an argon/krypton laser. Cells were viewed with an × 63/1.4 oil-immersion objective. The fluorescence of daunomycin incorporated into living cells incubated with 10 μM daunomycin for 1 h was visualized using the confocal microscope with an isothiocyanate (FITC) fluorescent set: λ$_{ex}$ = 488 nm, a 515 nm beam splitter and an emission band-pass filter set for FITC. Cells were incubated with 10 μM LysoSensor Green DND-189 (Molecular Probes, Eugene, OR, U.S.A.) for 30 min using the FITC fluorescence set. PKSV-PR$_{col50}$ cells were also incubated with 75 nM LysoTracker Red DND-99 (Molecular Probes) for 2 h, or with a conjugate of 50 μg/ml transferrin from human serum and Alexa fluor 568 (Molecular Probes) for 30 min as described [11], before being rinsed and incubated subsequently with daunomycin for 60 min. The red LysoTracker Red or Alexa fluor 568 emission was

viewed using the confocal microscope ($\lambda_{ex}$ = 568 nm). Emission light was passed through a 580 nm dichroic mirror and a 590 nm long-pass filter. The green daunomycin emission was viewed as described above, and the green and red emissions were collected using two photomultiplier tubes.

The grey-scale digital images were visualized with a 24-bit imaging system including Leica's Scanware software. The images generated passing through the middle plane of the nuclei were selected, imported into Adobe Photoshop 5.5 (Adobe, San Jose, CA, U.S.A.), pseudo-coloured, and in some cases overlapped to produce merged images. Quantitative analysis were performed using Metamorph 4.6 software (Universal Imaging Corp.). The relative mean fluorescence levels were obtain on a single-cell basis for each digital image. The lysosomal radius and number of lysosomes per cell were measured after segmentation, and regions of interest around these organelles were created. Segmentation required a series of consecutive image processing, including the application of a High Pass Fast Fourier Transform Filter, a morphometric classification to select individual round objects and the creation of a binary image mask.

### Lysosomal pH (pH$_{lys}$) recordings

pH$_{lys}$ in living cells was measured as described [11,19] using the pH-dependent fluorescent properties of FITC–dextrans incorporated into the lysosomes of living cells by fluid-phase endocytosis [20,21]. Briefly, confluent PKSV-PR and PKSV-PR$_{col50}$ cells grown on glass coverslips were incubated overnight at 37 °C with culture medium containing 1.5 mg/ml 10 kDa FITC–dextrans (Sigma, St. Louis, MO, U.S.A.). Cells were placed in a PDMI-2 temperature-controlled microincubator (Medical Systems Corp., Greenvale, NY, U.S.A.) mounted on the stage of an inverted microscope (Nikon Diaphot 300; Nikon Corp., Tokyo, Japan). Before measuring pH$_{lys}$, extracellular dye was removed by prolonged superfusion of the cells with dye-free medium at 37 °C. pH$_{lys}$ was measured after the FITC fluorescence signals had stabilized, during superfusion with a $CO_2$-free solution containing (in mM): 140 NaCl, 5 KCl, 0.4 $MgCl_2$, 1 $CaCl_2$, 10 D-glucose, 20 Hepes/NaOH, pH 7.4. FITC–dextran fluorescence was monitored using video-enhanced fluorescence microscopy and a BCECF [2′,7′-bis-(2-carboxyethyl)-5(6)-carboxyfluorescein] filter set [19], at 37 °C. After correction for shading, images pairs were ratioed on a pixel-by-pixel basis, and ratio values were converted into pH units using the in situ high K-nigericin method [22], over the 5.5–6.5 pH range, as described previously [19]. Background noise was not detectable. pH$_{lys}$ was measured using single cells (PKSV-PR$_{col50}$, $n$ = 62; PKSV-PR, $n$ = 330) from six to eight different passages.

### Percoll density-gradient fractionation

Confluent PKSV-PR and PKSV-PR$_{col50}$ cells were rinsed with ice-cold PBS containing 1 mM $CaCl_2$ and 1 mM $MgCl_2$, and then loaded with 2 $\mu$Ci/ml [G-$^3$H]daunomycin (specific radioactivity 5 Ci/mmol; NEN) for 60 min at 37 °C. Unloaded or daunomycin-loaded cells were washed with PBS and then once in ice-cold fractionation buffer (250 mM sucrose, 20 mM Hepes, 1 mM EDTA, pH 7.2) supplemented with 1 mM PMSF and 100 $\mu$g/ml protease inhibitor cocktail (Boehringer, Mannheim, Germany). Cells were scraped into 2 ml of fractionation buffer. Protein content was determined by the method of Lowry et al. [23] using BSA as standard. Cell homogenization was performed at 4 °C using a tight-fitting Dounce homogenizer (six passages). The resulting homogenate was centrifuged at 600 $g$ for 10 min at 4 °C. The supernatant was adjusted to 5 ml with fractionation buffer and then 3 ml of an 80% Percoll solution was added. The

gradient was performed by centrifuging for 35 min at 100 000 $g$ at 4 °C [24]. The fractions were collected from the bottom of the tubes using a needle, and the radioactivity was counted in aliquots (50 $\mu$l) of each fraction collected.

The NADPH:cytochrome $c$ reductase activity (used as a marker of the endoplasmic reticulum) and lysosomal mannosidase activity were determined for each fraction collected. NADPH:cytochrome $c$ reductase activity was measured in 50 mM phosphate/0.1 mM EDTA buffer, pH 7.7, using 1 mg/ml NADPH and 25 mg/ml cytochrome $c$ as substrates. Absorbance was measured at 550 nm. Lysosomal mannosidase activity was measured in 500 mM sodium acetate buffer, pH 4.5, using 10 mM $p$-nitrophenyl $\alpha$-D-mannopyranoside as substrate. Absorbance was measured at 410 nm.

### Drug resistance assay

Drug resistance was assayed using the MTT [3-(4,5-dimethylthiazol-2-yl)-2,5-diphenyltetrazolium bromide] dye assay [25]. Cells were seeded and grown in 96-well plates (8000 cells per well) for 2 days. The different agents to be tested were then added to the medium for 48 h. The medium was removed and replaced by 100 $\mu$l of MTT (400 $\mu$g/ml), and incubation was continued for 4 h at 37 °C. After centrifuging, the medium was removed, 100 $\mu$l of DMSO was added to each well and the plates were shaken for 10 min. Absorbance at 540 nm was determined for each well using a microplate autoreader (Titerteck Multiskan MC). IC$_{50}$ values, normalized against values obtained from cells incubated without drugs, were determined as described in [19].

### Statistical analysis

Results are reported as means ± S.E.M. from ($n$) experiments. Statistical differences between groups were assessed using Student's $t$ test. A $P$ value of < 0.05 was considered significant.

## RESULTS

### Daunomycin efflux and lysosomal enzyme secretion by drug-sensitive and drug-resistant renal epithelial cells

We have shown previously that PKSV-PR$_{col50}$ cells exhibit the typical features of MDR cells, including higher levels of mdr1b gene expression, than their drug-sensitive PKSV-PR counterparts, and high resistance to colchicine, vinblastine [19] and anthracyclines (the present study). The efflux of daunomycin was twice as great from PKSV-PR$_{col50}$ cells than from PKSV-PR cells preloaded with 100 nM [$^3$H]daunomycin for 60 min (Figure 1, left panel). The amount of daunomycin remaining in the cells after efflux was also significantly lower in PKSV-PR$_{col50}$ cells than in their drug-sensitive counterparts (Figure 1, right panel). The P-gp modulator verapamil (10 $\mu$M) did not affect the amount of daunomycin retained in the PKSV-PR cells, but significantly enhanced the cellular retention of the drug by PKSV-PR$_{col50}$ cells (2.7-fold; Figure 1, right panel). These results indicated that these MDR PKSV-PR$_{col50}$ cells retained less daunomycin and exhibited greater rates of drug efflux than their parent drug-sensitive PKSV-PR cells [19].

These MDR renal epithelial proximal tubule cells also exhibited changes in lysosomal structure. As reported by Beck [26], more abundant intracellular acidic vesicular structures that accumulated 9-aminoacridine and FITC–dextrans were detected in PKSV-PR$_{col50}$ cells than in PKSV-PR cells [19]. To analyse further the acidic compartments of these drug-sensitive and drug-resistant renal cells, imaging studies were performed using the lysosomotropic agent LysoSensor Green DND-189. The
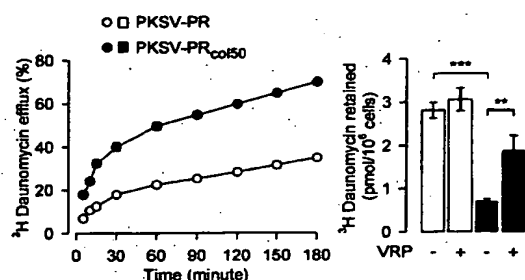
**Figure 1    Efflux and retention of daunomycin in drug-sensitive and drug-resistant renal proximal tubule cells**

Confluent cells were loaded with 100 nM [G-$^3$H]daunomycin for 60 min at 37 °C and washed with ice-cold serum-free medium. Left panel: the efflux of daunomycin, expressed as a percentage of the total radioactivity incorporated, was measured over 3 h. Right panel: the bars represent the cellular content of [G-$^3$H]daunomycin (expressed as pmol/$10^6$ cells) remaining after the 3 h efflux measured in the absence (−) or presence (+) of 10 $\mu$M verapamil (VRP) in PKSV-PR cells (□) and PKSV-PR$_{col50}$ cells (■). Values are the means ± S.E.M. from five separate experiments; **$P < 0.01$, ***$P < 0.001$.

fluorescence of LysoSensor Green is pH-dependent, and increases as the pH decreases. PKSV-PR cells exhibited a discrete punctuate LysoSensor Green fluorescence, distributed throughout the cytoplasm (Figure 2A), whereas PKSV-PR$_{col50}$ cells exhibited numerous, densely packed fluorescence signals concentrated near the nucleus (Figure 2C). Quantitative analysis of these fluorescence signals revealed that the number of LysoSensor Green-labelled organelles (i.e. lysosomes) per cell was 1.8-fold greater in PKSV-PR$_{col50}$ than in PKSV-PR cells (Figure 2E). The mean radius of the fluorescent vesicles (ranging between 235 and 364 nm) was also slightly greater in drug-resistant PKSV-PR$_{col50}$ cells than in their drug-sensitive PKSV-PR counterparts (Figure 2E). Similar results were obtained by using the pH-independent LysoTracker Red DND-99 (results not shown). Although one cannot exclude the possibility that the incorporation of the fluorescent dyes induced swelling of the organelles, leading to an overestimation of the size of the labelled organelles, these results were in accordance with our previous observations using 9-aminoacridine and FITC–dextrans [19]. The fact that there was no major difference in the intensity of the signals provided by the pH-dependent LysoSensor Green signals in PKSV-PR and PKSV-PR$_{col50}$ cells (Figure 2F) also suggested that the lysosomes from drug-resistant and drug-sensitive renal cells exhibited a normal acidic pH. Vacuolar H$^+$-ATPases contribute to the acidification of a variety of intracellular organelles in eukaryotic cells [27]. They are also highly expressed in endosomes and lysosomes of proximal tubule cells [28,29]. Cells were therefore incubated with CCM A, a potent vacuolar H$^+$-ATPase inhibitor that does not affect ATP levels [30,31], to evaluate the vacuolar H$^+$-ATPase-dependent acidification of lysosomes in PKSV-PR and PKSV-PR$_{col50}$ cells. The addition of 50 nM CCM A to the medium bathing the cells loaded with the LysoSensor Green induced within 15 min a substantial decrease in the intensity of the fluorescence signals in both PKSV-PR (−75 %) and PKSV-PR$_{col50}$ (−65 %) cells (Figure 2F), leading to almost complete disappearance of the green fluorescence from both cell types (Figures 2B and 2D). Overall, these results strongly suggest that PKSV-PR$_{col50}$ cells have an expanded functional acidic lysosomal compartment.

We next performed pH measurements to estimate pH$_{lys}$. As reported for drug-sensitive MCF-7 breast cancer cells [11], we
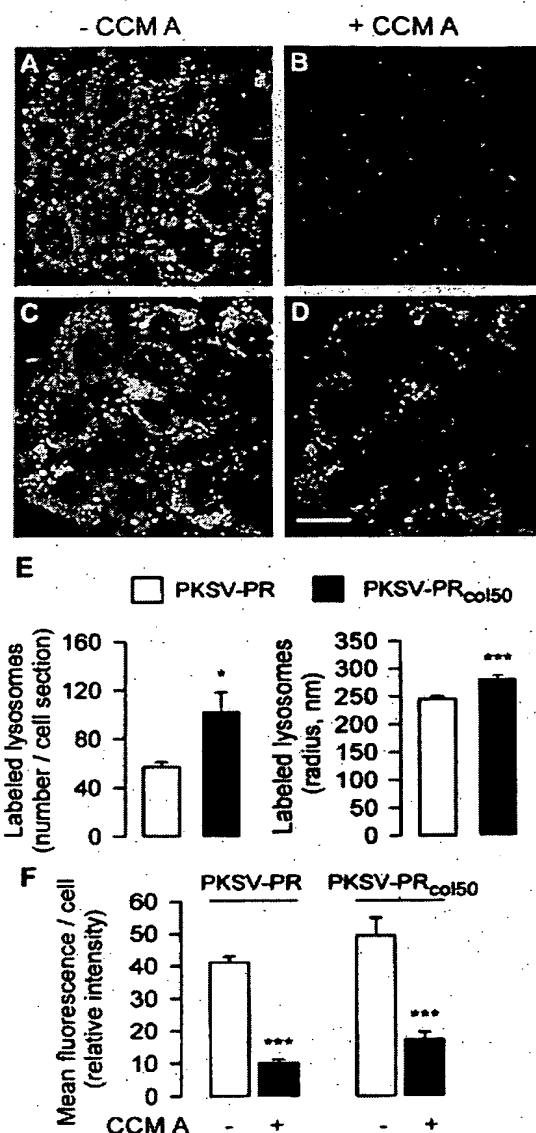
**Figure 2    LysoSensor Green labelling of acidic compartments of PKSV-PR and PKSV-PR$_{col50}$ cells**

Shown is the fluorescence of PKSV-PR (A, B) and PKSV-PR$_{col50}$ (C, D) cells incubated with LysoSensor Green dye used to label the lysosomes. Untreated PKSV-PR$_{col50}$ cells (C) exhibited more numerous punctate cytoplasmic organelles than PKSV-PR cells (A). CCM A (20 nM for 15 min) induced a rapid decrease in pH-dependent LysoSensor Green labelling in both PKSV-PR (B) and PKSV-PR$_{col50}$ (D) cells. Scale bar = 10 $\mu$M. The density and radius of lysosomes labelled with the LysoSensor Green fluorescent dye (E) and the mean LysoSensor Green fluorescence intensity per cell (F) were quantified from confocal laser scanning inverted microscopy images of passing through the middle plane of the nuclei of PKSV-PR and PKSV-PR$_{col50}$ cells, as described in the Materials and methods section. Values are the means ± S.E.M. from individual cells analysed using images (11–20 cells per image) generated by confocal laser scanning inverted microscopy from three or four separate experiments for each condition tested. Significance of differences: *$P < 0.05$, ***$P < 0.001$.
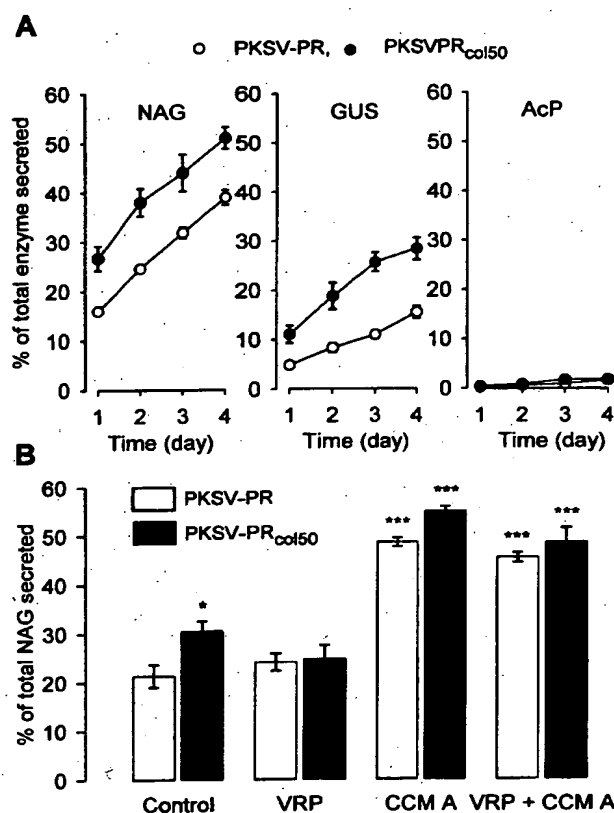
**A**

o  PKSV-PR,  ●  PKSVPR$_{col50}$



**B**



**Figure 3  Rates of secretion of lysosomal enzymes by drug-sensitive and drug-resistant renal proximal tubule cells**

(A) The percentages of total NAG, $\beta$-glucuronidase (GUS) and AcP secreted by PKSV-PR cells (O) and PKSV-PR$_{col50}$ cells (●) were measured 1–4 days after confluency. Values are the means ± S.E.M. from six separate experiments. The percentages of secreted NAG and $\beta$-glucuronidase were significantly higher in PKSV-PR$_{col50}$ cells than in PKSV-PR cells ($P < 0.01$). (B) The percentage of total NAG secreted was measured in confluent PKSV-PR cells (□) and PKSV-PR$_{col50}$ cells (■) incubated without (Control) or with 10 $\mu$M verapamil (VRP), 20 nM CCM A or verapamil plus CCM A for 24 h. Values are the means ± S.E.M. from five separate experiments; $^{*}P < 0.05$, $^{***}P < 0.001$ compared with control values.
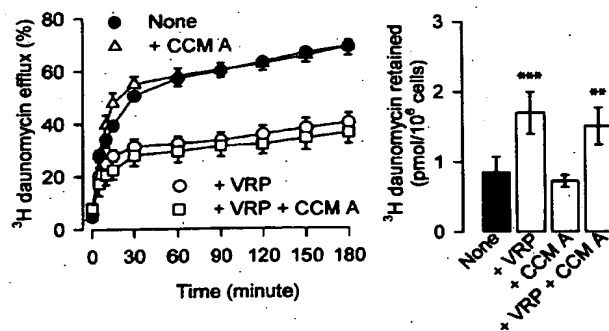


**Figure 4  Different effects of verapamil and CCM A on daunomycin efflux from drug-resistant PKSV-PR$_{col50}$ cells**

Left panel: the efflux and the cellular retention of [G-$^3$H]daunomycin were measured in PKSV-PR$_{col50}$ cells incubated without (●) or with verapamil (VRP; 10 $\mu$M; O), CCM A (50 nM; $\triangle$) or verapamil plus CCM A (□) for 24 h at 37 °C. Cells were then loaded with 100 nM [G-$^3$H]daunomycin as described in the legend of Figure 1, and daunomycin efflux was measured over 3 h. Right panel: the bars represent the cellular content of [G-$^3$H]daunomycin remaining after the 3 h efflux measured in the absence (None) and presence of verapamil, CCM A or verapamil + CCM A. Values are the means ± S.E.M. from five separate experiments; $^{**}P < 0.01$, $^{***}P < 0.001$ compared with untreated cells ('None').

failed to obtain a correct measurement of pH$_{lys}$ in the drug-sensitive PKSV-PR cells by using the pH-dependent LysoSensor Green DND-189. However, the results from the fluorescence studies showing that CCM A decreased the intensity of the pH-dependent LysoSensor Green DND-189 signal strongly suggested that the lysosomes from the parent, drug-sensitive PKSV-PR cells were acidic. Indeed, pH measurements using endocytosed 10 kDa FITC–dextrans revealed that the drug-resistant PKSV-PR$_{col50}$ cells had a slightly, but not significantly, lower resting pH$_{lys}$ (5.66 ± 0.02) than drug-sensitive PKSV-PR cells (5.74 ± 0.02).

The activities of cellular and secreted lysosomal enzymes in PKSV-PR cells and PKSV-PR$_{col50}$ cells were then measured to find out whether the rates of secretion of lysosomal enzymes were higher in drug-resistant renal proximal tubule cells, as has been reported for CEM/VLB$_{100}$ lymphoblastic cells [32]. The percentages of secreted NAG and $\beta$-glucuronidase were 1.3-fold and 1.8-fold greater respectively in PKSV-PR$_{col50}$ cells than in PKSV-

PR cells, whereas the percentage of secreted AcP remained low ($< 2\%$) after 4 days, and was similar in PKSV-PR and PKSV-PR$_{col50}$ cells (Figure 3A). CCM A (20 nM) stimulated the percentage of secreted NAG recovered from the culture medium after 24 h for both PKSV-PR (2.2-fold) and PKSV-PR$_{col50}$ (1.8-fold) cells (Figure 3B). In contrast, verapamil (10 $\mu$M) did not alter the level of secreted NAG in either untreated or CCM A-treated drug-sensitive or -resistant cells (Figure 3B). This raises the question of whether the rapid alkalinization of the lysosomes induced by lysosomotropic agents, responsible for an increase in the secretion of lysosomal enzymes [16,33–35], could also affect the P-gp-dependent efflux of daunomycin from drug-resistant PKSV-PR$_{col50}$ cells. The rate of [$^3$H]daunomycin efflux was almost identical in PKSV-PR$_{col50}$ cells incubated without or with 20 nM CCM A (Figure 4, left panel). Moreover, CCM A did not significantly alter the rate of daunomycin efflux or the amount of drug remaining after efflux in either untreated or verapamil-treated PKSV-PR$_{col50}$ cells (Figure 4, right panel).

**Cellular distribution of daunomycin in drug-sensitive and -resistant renal epithelial cells**

Cell imaging studies were performed to find out whether the subcellular distribution of daunomycin differed in drug-sensitive and drug-resistant proximal tubule cells. Daunomycin was widely distributed throughout the cytoplasm, in a few intracellular vesicular structures and in the nuclei of drug-sensitive PKSV-PR cells (Figure 5A), whereas in PKSV-PR$_{col50}$ cells it was barely detectable in the cytosol and nuclei, but was concentrated in round structures around the nuclei (Figure 5G). Sequential labelling with the pH-insensitive LysoTracker Red DND-99 lysosomal marker and daunomycin showed that daunomycin was always co-localized with the lysosome-specific fluorescent dye (Figures 5C and 5D). In contrast, daunomycin did not co-localize with the transferrin–Alexa fluor 568 conjugate used to label the recycling endocytic compartment (Figures 5E and 5F).
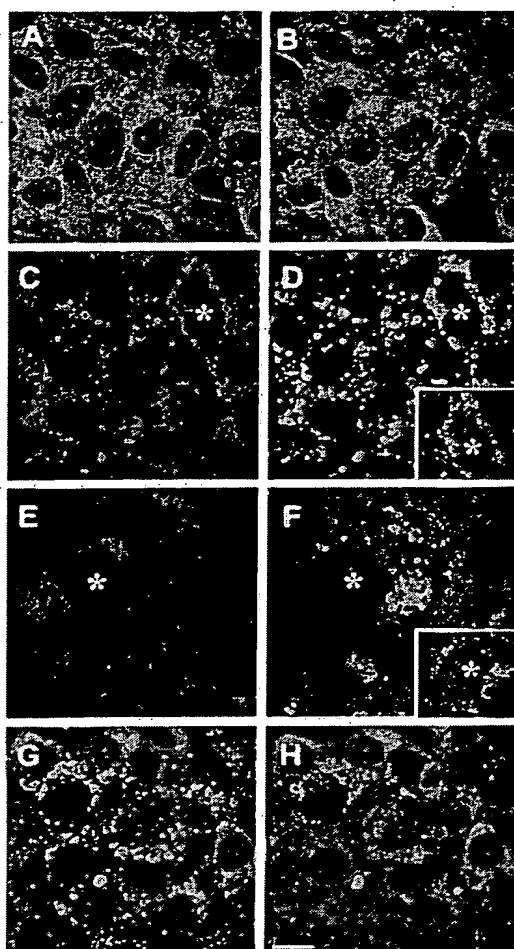
**Figure 5    Daunomycin distribution in drug-sensitive and drug-resistant renal proximal tubule cells**

The pattern of daunomycin labelling (in green) was analysed by confocal laser scanning inverted microscopy in confluent living PKSV-PR cells (A, B) and PKSV-PR$_{col50}$ cells (G, H) incubated without or with CCM A (50 nM for 15 min), and in PKSV-PR$_{col50}$ cells incubated sequentially with LysoTracker Red DND-99 (C, D) or with the transferrin–Alexa fluor 568 conjugate (E, F) and daunomycin, as described in the Materials and Methods section. The fluorescence of daunomycin, widely distributed throughout the cytoplasm and nucleoplasm (A), was not altered by CCM A (B). The punctate fluorescence of LysoTracker Red DND-99 in PKSV-PR$_{col50}$ cells (C) exactly matched the distribution of daunomycin (D, and inset), whereas the fluorescence of the transferrin–Alexa fluor 568 conjugate (E) did not co-localize with daunomycin (F, and inset). Daunomycin accumulated in the lysosomes from PKSV-PR$_{col50}$ cells (G) was rapidly redistributed within the cytoplasm after addition of 20 nM CCM A for 15 min (H). Insets, "merge images. Scale bar = 10 $\mu$m.

**Effect of CCM A on the lysosomal accumulation of daunomycin in drug-resistant renal epithelial cells**

Alkalinization of the lysosomal compartment by CCM A (20 nM for 15 min) did not significantly alter the nucleo-cytoplasmic distribution of daunomycin in PKSV-PR cells (Figure 5B), but did induce a marked decrease in the punctate fluorescence of the drug accumulated in lysosomes in PKSV-PR$_{col50}$ cells (Figure 5H). Percoll density-gradient fractionation, which is able to
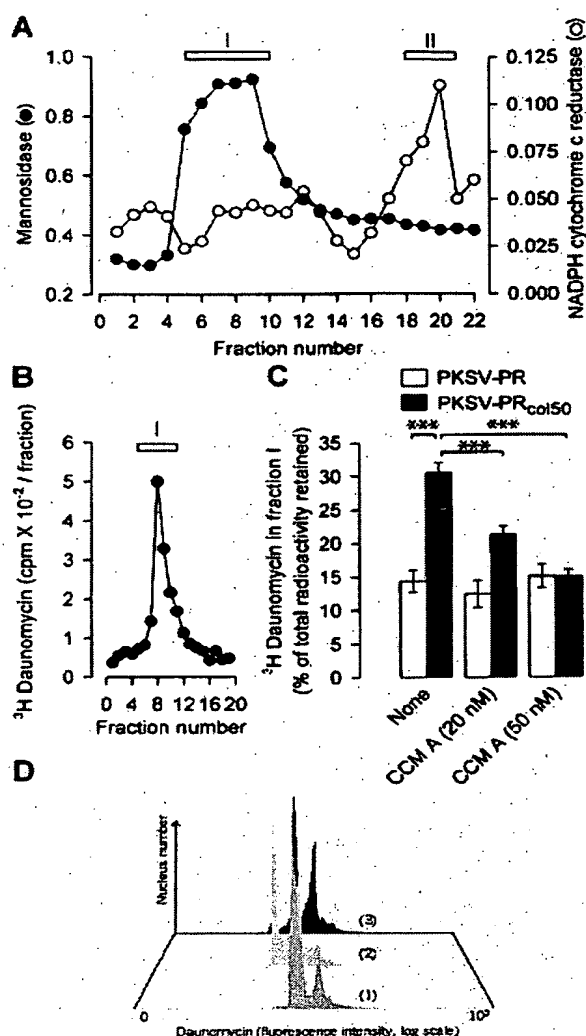
**Figure 6    Lysosomal accumulation of daunomycin, and nuclear redistribution induced by CCM A**

(A) Percoll density gradient fractionation was performed on homogenates of unloaded or [G-$^3$H]daunomycin-loaded (2 $\mu$Ci/ml for 60 min) cells, as described in the Materials and methods section. The profiles of lysosomal mannosidase and NADPH:cytochrome $c$ reductase activities revealed two fractions: one highly enriched with lysosomes (fraction I) and the other with endoplasmic reticulum (fraction II). (B) A sharp peak of [G-$^3$H]daunomycin was detected in fraction I of the PKSV-PR$_{col50}$ cells. (C) The relative percentage of [G-$^3$H]daunomycin accumulated in fraction I decreased significantly after addition of 20–50 nM CCM A during the loading period in PKSV-PR$_{col50}$ cells, but remained unchanged in PKSV-PR cells; ***$P < 0.001$. (D) Three-dimensional galley plots of fluorescent daunomycin intensity analysed by flow cytometry in isolated nuclei from untreated PKSV-PR cells (1), untreated PKSV-PR$_{col50}$ cells (2) and CCM A-treated PKSV-PR$_{col50}$ cells (3). The main fluorescence peak corresponded to nuclei in $G_0/G_1$ phase.

resolve lysosomes from the endoplasmic reticulum, was then performed to measure drug accumulation in the lysosomal compartments of PKSV-PR and PKSV-PR$_{col50}$ cells loaded with 2 $\mu$Ci/ml [G-$^3$H]daunomycin for 60 min at 37 °C (Figure 6). The profiles of lysosomal mannosidase and NADPH:cytochrome $c$
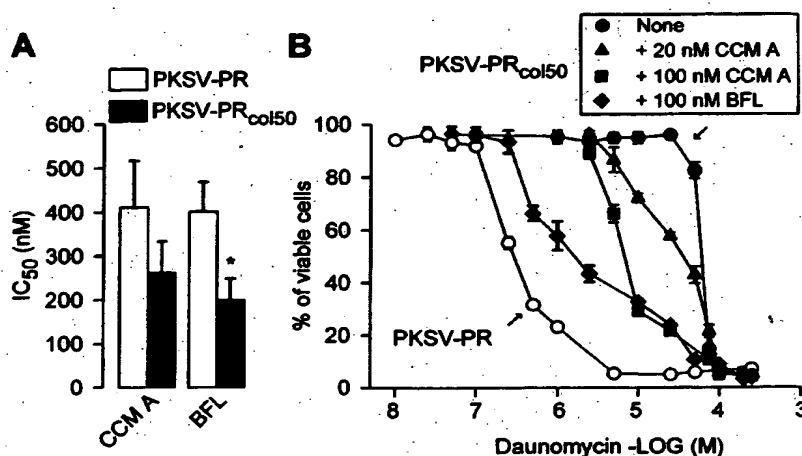
**Figure 7    Effects of CCM A and bafilomycin A1 on daunomycin sensitivity of drug-sensitive and drug-resistant renal proximal tubule cells**

The sensitivity of the parent PKSV-PR cells and selected PKSV-PR$_{col50}$ cells to CCM A, bafilomycin A1 (BFL) and daunomycin was determined by using the MTT assay after exposure to the drugs for 48 h. (A) IC$_{50}$ values for CCM A and bafilomycin A1. (B) The percentage of viable cells was measured in untreated PKSV-PR cells and in untreated or CCM A- or bafilomycin A1-treated PKSV-PR$_{col50}$ cells incubated with increasing concentrations of daunomycin for 48 h. Values are the means ± S.E.M. from six to eight separate experiments; *$P < 0.05$.

reductase activities revealed two main fractions, one highly enriched with lysosomes (fraction I) and the other with endoplasmic reticulum (fraction II) (Figure 6A). Consistent with the fluorescence studies, a sharp peak of [G-$^3$H]daunomycin was recovered from the lysosome-enriched fraction I from PKSV-PR$_{col50}$ cells (Figure 6B). Parent PKSV-PR cells exhibited a similar profile of daunomycin distribution (results not shown), but the percentage of radioactivity incorporated into cells and recovered from the lysosome-enriched fraction I was only about half as great for PKSV-PR cells as for PKSV-PR$_{col50}$ cells (Figure 6C). Adding 20 nM or 50 nM CCM A to the culture medium during the loading period produced a significant and dose-dependent decrease in the percentage of [G-$^3$H]daunomycin recovered from the lysosome-enriched fraction I of the PKSV-PR$_{col50}$ cells, but not of the PKSV-PR cells (Figure 6C). The results from flow cytometry also showed that the fluorescence intensity of daunomycin accumulated in isolated nuclei from untreated PKSV-PR cells was about twice as great as that in nuclei from untreated PKSV-PR$_{col50}$ cells (Figure 6D). Conversely, preincubating PKSV-PR$_{col50}$ cells with CCM A (20 nM for 24 h), which significantly decreased the amount of daunomycin accumulated in the lysosomes (Figure 6C), caused a 2.2-fold increase in the nuclear fluorescent daunomycin intensity as compared with that in untreated PKSV-PR$_{col50}$ cells (Figure 6D).

**Inhibitors of the vacuolar proton pump restore the sensitivity of MDR renal epithelial cells to anthracyclines**

The disruption of lysosomal acidification by CCM A caused a marked nuclear redistribution of daunomycin in the drug-resistant PKSV-PR$_{col50}$ cells, without increasing the cellular efflux of the chemotherapeutic drug (see Figure 4). This raises the question of whether proton pump inhibitors also restore the sensitivity of PKSV-PR$_{col50}$ cells to anthracyclines. Cells were first tested for their sensitivity to proton pump inhibitors. The results from the MTT assay showed that PKSV-PR$_{col50}$ cells are about twice as sensitive to CCM A and bafilomycin A1 as PKSV-PR cells (Figure 7A). However, the concentrations of CCM A and bafilomycin A1 used (20–100 nM) did not alter cell viability

**Table 1    Effects of CCM A and bafilomycin A1 on relative resistance to anthracyclines**

PKSV-PR and PKSV-PR$_{col50}$ cells seeded on 96-well trays were incubated with 10 $\mu$M daunomycin, doxorubicin or epirubicin and without or with 20 nM CCM A or bafilomycin A1 (BFL) for 48 h. IC$_{50}$ values were determined using the MTT colorimetric assay, and were normalized against values obtained from cells incubated without drugs. Values are the means ± S.E.M. from ($n$) separate experiments. Fold resistance corresponds to the mean ratio of the IC$_{50}$ values of PKSV-PR$_{col50}$ cells over those for PKSV-PR cells.

| Treatment | IC$_{50}$ | | Fold resistance |
|---|---|---|---|
| | PKSV-PR cells | PKSV-PR$_{col50}$ cells | |
| Daunomycin | 0.6 ± 0.2 (8) | 57.7 ± 2.3 (6) | 96.2 |
| + CCM A (20 nM) | 1.4 ± 0.1 (6) | 23.7 ± 1.1 (7) | 16.9 |
| + BFL (20 nM) | 1.0 ± 0.3 (5) | 5.2 ± 1.2 (6) | 5.2 |
| Doxorubicin | 12.3 ± 1.9 (9) | 375.7 ± 38.7 (9) | 30.5 |
| + CCM A (20 nM) | 9.6 ± 2.1 (8) | 14.2 ± 4.4 (6) | 1.5 |
| + BFL (20 nM) | 10.1 ± 1.4 (8) | 17.9 ± 14.9 (6) | 1.8 |
| Epirubicin | 21.0 ± 1.8 (8) | 118.9 ± 14.9 (9) | 5.7 |
| + CCM A (20 nM) | 9.5 ± 1.0 (8) | 7.3 ± 0.4 (8) | 0.8 |
| + BFL (20 nM) | 15.9 ± 3.2 (6) | 8.2 ± 2.0 (6) | 0.5 |

(> 90 % viable cells) in either drug-sensitive or -resistant cells. Preincubating the cells with non-cytotoxic concentrations of CCM A (20–100 nM) or bafilomycin A1 (100 nM) restored the sensitivity of the PKSV-PR$_{col50}$ cells to daunomycin, to levels close to that measured in their drug-sensitive PKSV-PR counterparts (Figure 7B). Adding 20 nM CCM A or bafilomycin A1 to the culture medium did not increase the cytotoxicity of anthracyclines in PKSV-PR cells (Table 1). In contrast, both vacuolar H$^+$-ATPase inhibitors dramatically lowered the resistance of PKSV-PR$_{col50}$ cells to daunomycin, and completely restored their sensitivity to doxorubicin and epirubicin to the same levels as in parent PKSV-PR cells (Table 1). These findings demonstrate that inhibitors of vacuolar H$^+$-ATPase induced a nucleo-cytoplasmic redistribution of weak-base daunomycin within drug-

resistant PKSV-PR$_{col50}$ cells, and restored the sensitivity of these drug-resistant renal epithelial proximal tubule cells to daunomycin, doxorubicin and epirubicin.

## DISCUSSION

The findings of the present study show that daunomycin is sequestered in the acidic lysosomes of MDR renal proximal tubule cells, and that inhibitors of proton pumps cause a rapid redistribution of the drug in the cytoplasm and nucleus. In addition, both CCM A and bafilomycin A1 restore the sensitivity of the drug-resistant cells to anthracyclines. The contribution of the intracellular trapping of drugs to the MDR phenomenon is under debate [11,12,14]. The findings of the present study strongly suggest that the sequestration of weak-base therapeutic drugs in acidic organelles does indeed contribute to the acquired drug resistance phenotype of MDR epithelial renal cells. The results from fluorescence studies of living cells reveal that daunomycin is detected mainly, if not exclusively, in the lysosomes of drug-resistant PKSV-PR$_{col50}$ cells. Although several authors have reported that anthracylines can be detected in other acidic compartments, such as the *trans*-Golgi network or recycling endosomes [7,9,11], all of the fluorescent drugs tested have always been found solely in the more acidic lysosomal compartment of the various MDR cell lines analysed [7–11].

It has been suggested that the intracellular trapping of drugs in the expanded acidic organelle compartments of drug-resistant cells [10,26], plus the active drug export mediated by membranous ATP-dependent P-gps or MRPs, contributes to the reduced accumulation of drugs in MDR cells. Altan et al. [11] have reported that lysosomes and recycling endosomes are not acidified in drug-sensitive MCF-7 breast tumour cells, and that the cytosol of drug-sensitive MCF-7 cells is more acidic than the cytosol of their drug-resistant MCF-7/ADR counterparts [11]. Thus the increase in the pH gradient between the cytosol and acidic organelle compartments in MCF-7/ADR drug-resistant cells favours the protonation and sequestration of weak-base anthracyclines (with a p$K_a$ of around 8) in acidic organelles. As in many MDR tumour cells [36], we also found that the intracellular pH of drug-resistant PKSV-PR$_{col50}$ cells is slightly higher than that of the parent PKSV-PR cells [19]. However, in contrast with the situation reported for drug-sensitive and -resistant MCF-7 cells, the lysosomal compartments of drug-sensitive and -resistant renal proximal tubule cells exhibited quite similar acidic pH$_{lys}$ values. The results from the pH$_{lys}$ values measured using pH-sensitive FITC–dextrans incorporated into the lysosomes by fluid-phase endocytosis [20,21] were in complete accordance with the relative fluorescence intensities provided by the pH-dependent LysoSensor Green DND-189 dye. Parent PKSV-PR cells and drug-resistant PKSV-PR$_{col50}$ cells exhibited similar acidic pH$_{lys}$ values, and were both sensitive to the action of CCM A (see Figure 2). These findings therefore indicate that the lysosomes of the parent drug-sensitive, but non-tumoral, PKSV-PR cells did not fail to acidify like the drug-sensitive MCF-7 cells. Weak-base anthracycines are thought to enter P-gp-expressing cells by pinocytosis and then accumulate passively in the acidic compartments [37]. Thus the greater lysosomal accumulation of daunomycin in drug-resistant PKSV-PR$_{col50}$ cells is consistent with an expanded lysosomal compartment. The fact that CCM A also inhibits the accumulation of daunomycin in lysosomes from PKSV-PR$_{col50}$ cells is consistent with the view that this accumulation is passive and requires acidic lysosomes.

Consistent with their greater content of acidic lysosomal vesicles, the drug-resistant PKSV-PR$_{col50}$ cells exhibited increased levels of secreted NAG and $\beta$-glucuronidase lysosomal enzymes.

Similar results have been reported in MDR human CEM/VLB$_{100}$ lymphoblastic cells [32]. These effects appear to be specific for lysosomal enzymes that require the mannose-6-phosphate receptor to be targeted in lysosomes [38,39], since the rate of secretion of AcP, which does not require the mannose-6-phosphate receptor [40], remained low and identical in PKSV-PR and PKSV-PR$_{col50}$ cells. Interestingly, CCM A, which stimulates the secretion of NAG and $\beta$-glucuronidase in both untreated and verapamil-treated PKSV-PR$_{col50}$ cells to the same extent, had no effect on the P-gp-dependent secretion of daunomycin. These findings indicate that the rapid alkaline shift of the lysosome induced by CCM A does not stimulate the apical P-gp-dependent secretion of daunomycin.

Thus the abundance of functional acidic lysosomes promotes the lysosomal trapping of protonated anthracyclines in MDR PKSV-PR$_{col50}$ cells. Agents such as protonophores, the weak base chloroquine or inhibitors of the vacuolar H$^+$-ATPase that block the acidification of organelles allow the release of anthracyclines from acidic organelles and lead to a substantial accumulation of the drugs in the cytosol and nucleus of MDR cells [10,11]. This enhanced accumulation of the drugs in the cytosol and nucleus should directly affect the cytotoxic nuclear effect of anthracyclines [13]. Our data now provide direct evidence that the inhibition of the vacuolar H$^+$-ATPase by CCM A and bafilomycin A1 almost completely abolishes resistance to daunomycin, doxorubicin and epirubicin in the MDR PKSV-PR$_{col50}$ cell line. CCM A does not affect the verapamil-dependent cellular efflux of daunomycin, and so the primary mode of action of vacuolar H$^+$-ATPase inhibitors does not seem to require an intracellular P-gp. The fact that the IC$_{50}$ values for CCM A and bafilomycin A1 are lower in PKSV-PR$_{col50}$ cells than in PKSV-PR cells also may suggest that the drug-resistant cells overexpress vacuolar proton pumps. The acidic pH of vesicles is generated by vacuolar H$^+$-ATPases that actively translocate protons across the organelle membranes. The differences between the steady-state pH of endocytic and secretory organelles (lysosomes being the most acidic compartment in the endocytic pathway) reflect differences in the regulation of organelle pumps and conductances [41]. Further studies will be needed to find out whether the loss of acidification observed in some drug-sensitive tumour cells is due to a defect in the density or assembly of the vacuolar H$^+$-ATPase and/or whether, conversely, vacuolar proton pumps are overexpressed in MDR cells, as has been reported for MDR HL60 cells [42]. In conclusion, the findings of the present study provide direct evidence that the acidic lysosomal compartment of MDR cells offers a potential site for the reversal of anthracycline resistance by lysosomotropic agents.

## REFERENCES

1   Endicott, J. A. and Ling, V. (1989) The biochemistry of P-glycoprotein mediated multidrug resistance. Annu. Rev. Biochem. **58**, 137–171

2   Gottesman, M. M. and Pastan, I. (1993) Biochemistry of multidrug resistance mediated by the multidrug transporter. Annu. Rev. Biochem. **62**, 385–427

3   Simon, M. and Schindler, M. (1994) Cell biological mechanisms of multidrug resistance in tumors. Proc. Natl. Acad. Sci. U.S.A. **9**, 3497–3504

4   Hoffman, M. M., Wei, L. Y. and Roepe, R. D. (1996) Are altered pHi and membrane potential in hu MDR1 transfectants sufficient to cause MDR protein-mediated multidrug resistance? J. Gen. Physiol. **108**, 295–313

5   Wadkins, R. M. and Roepe, P. D. (1997) Biophysical aspects of P-glycoprotein-mediated multidrug resistance. Int. Rev. Cytol. **171**, 121–165

6   Hindenburg, A. A., Gervasoni, Jr, J. E., Krisna, S., Stewart, V. J., Rosado, M. L. J., Bhalla, K., Baker, M. A. and Taub, R. N. (1989) Intracellular distribution and pharmacokinetics of daunorubicin in anthracycline-sensitive and -resistant HL-60 cells. Cancer Res. **49**, 4607–4614

7   Coley, H. M., Amos, W. B., Twentyman, P. R. and Workman, P. (1993) Examination by laser scanning confocal fluorescence imaging microscopy of the subcellular localisation of anthracyclines in parent and multidrug resistant cell lines. Br. J. Cancer **67**, 1316–1323

8   Rutherford, A. V. and Willingham, M. C. (1993) Ultrastructural localization of daunomycin in multidrug-resistant cultured cells with modulation of the multidrug transporter. J. Histochem. Cytochem. **41**, 1573–1577

9   Lautier, D., Bailly, J. D., Demur, C., Herbert, J. M., Bousquet, C. and Laurent, G. (1997) Altered intracellular distribution of daunorubicin in immature acute myeloid leukemia cells. Int. J. Cancer **71**, 292–299

10  Hurwitz, S. J., Terashima, M., Mizunuma, N. and Slapak, C. A. (1997) Vesicular anthracycline accumulation in doxorubicin-selected U-937 cells: participation of lysosomes. Blood **89**, 3745–3754

11  Altan, N., Chen, Y., Schindler, M. and Simon, S. M. (1998) Defective acidification in human breast tumor cells and implications for chemotherapy. J. Exp. Med. **187**, 1583–1589

12  Schindler, M., Grabski, S., Hoof, E. and Simon, S. M. (1996) Defective pH regulation of acidic compartments in human breast cancer cells (MCF-7) is normalized in adriamycin-resistant cells (MCF-7adr). Biochemistry **35**, 2811–2817

13  Gewirtz, D. A. (1999) A critical evaluation of the mechanisms of action proposed for the antitumor effects of the anthracycline antibiotics adriamycin and daunorubicin. Biochem. Pharmacol. **57**, 727–741

14  Wang, E., Lee, M. D. and Dunn, K. W. (2000) Lysosomal accumulation of drugs in drug-sensitive MES-SA but not multidrug-resistant MES-SA/Dx5 uterine sarcoma cells. J. Cell. Physiol. **184**, 263–274

15  Thiebaut, F., Tsuruo, T., Hamada, H., Gottesman, M. M., Pastan, I. and Willingham, M. C. (1987) Cellular localization of the multidrug-resistant gene product P-glycoprotein in normal human tissues. Proc. Natl. Acad. Sci. U.S.A. **84**, 7735–7738

16  Riccaldi, D., Robic, D., Bens, M., Cluzeaud, F., Wu, M. S., Bourbouze, R. and Vandewalle, A. (1995) Cultured proximal cells derived from transgenic mouse provide model to study drug toxicity. Kidney Int. **48**, 722–730

17  Cartier, N., Lacave, R., Vallet, V., Hagege, R., Hellio, J., Robine, S., Pringault, E., Cluzeaud, F., Briand, P., Kahn, A. and Vandewalle, A. (1993) Establishment of proximal tubule cell lines by targeted oncogenesis in transgenic mice using the L-pyruvate kinase-SV40 (T) antigen hybrid gene. J. Cell Sci. **104**, 695–704

18  Vandewalle, A. (1999) Immortalized kidney cells derived from transgenic mice harboring L-type pyruvate kinase and vimentin promoters. Exp. Nephrol. **7**, 386–393

19  Lacave, R., Ouar, Z., Paulais, M., Bens, M., Ricci, S., Cluzeaud, F. and Vandewalle, A. (1999) Lysosomotropic agents increase vinblastine efflux from mouse MDR proximal kidney cells exhibiting vectorial drug transport. J. Cell. Physiol. **178**, 247–257

20  Ohkuma, S. and Poole, B. (1978) Fluorescence probe measurement of the intralysosomal pH in living cells and the perturbation of pH by various agents. Proc. Natl. Acad. Sci. U.S.A. **75**, 3327–3331

21  Jiang, L. W., Maher, V. M., McCormick, J. J. and Schindler, M. (1990) Alkalinization of the lysosomes is correlated with *ras* transformation of murine and human fibroblasts. J. Biol. Chem. **265**, 4775–4777

22  Thomas, J. A. (1979) Intracellular pH measurements in Ehrlich ascites tumor cells utilizing spectroscopic probes generated in situ. Biochemistry **18**, 2210–2218

23  Lowry, O. H., Rosebrough, N. J., Farr, A. L. and Randall, J. R. (1951) Protein measurements with the folin phenol reagent. J. Biol. Chem. **193**, 265–275

24  Saint-Pol, A., Bauvy, C., Codogno, P. and Moore, S. E. (1997) Transfer of free polymannose-type oligosaccharides from the cytosol to lysosomes in cultured human hepatocellular carcinoma HepG2 cells. J. Cell Biol. **136**, 45–59

25  Carmichael, J. and Degraff, W. G. (1987) Evaluation of tetrazolium based semiautomatized colorimetric assay: assessment of chemosensitivity testing. Cancer Res. **47**, 936–942

26  Beck, W. T. (1997) The cell biology of multiple drug resistance. Biochem. Pharmacol. **36**, 2879–2887

27  Stevens, T. H. and Forgac, M. (1997) Structure, function and regulation of the vacuolar (H⁺)-ATPase. Annu. Rev. Cell Dev. Biol. **13**, 779–808

28  Gluck, S. L, Underhill, D. M., Iyori, M., Holliday, L. S., Kostrominova, T. Y. and Lee, B. S. (1996) Physiology and biochemistry of the kidney vacuolar H⁺-ATPase. Annu. Rev. Physiol. **58**, 427–445

29  Günther, W., Lüchow, A., Cluzeaud, F., Vandewalle, A. and Jentsch, T. J. (1998) ClC-5, the chloride channel mutated in Dent's disease, colocalizes with the proton pump in endocytotically active kidney cells. Proc. Natl. Acad. Sci. U.S.A. **95**, 8075–8080

30  Woo, J.-T., Shinohara, C., Sakai, K., Hasumi, K. and Endo, A. (1992) Isolation, characterization and biological activities of concanamycins as inhibitors of lysosomal acidification. J. Antibiot. **45**, 1108–1116

31  Kataoka, T., Muroi, M., Ohkuma, S., Waritani, T., Magae, J., Takatsuki, A., Kondo, S., Yamasaki, M. and Nagai, K. (1995) Prodigiosin 25-C uncouples vacuolar type H⁺-ATPase; inhibits vacuolar acidification and affects glycoprotein processing. FEBS Lett. **359**, 53–59

32  Warren, L., Jardillier, J. C. and Ordentlich, P. (1991) Secretion of lysosomal enzymes by drug-sensitive and multiple drug-resistant cells. Cancer Res. **51**, 1996–2001

33  Gonzalez-Noriega, A., Grubb, J. H., Talkad, V. and Sly, W. S. (1980) Chloroquine inhibits lysosomal enzyme pinocytosis and enhances lysosomal enzyme secretion by impairing receptor recycling. J. Cell Biol. **85**, 839–852

34  Riches, D. W. and Stanworth, D. R. (1980) Primary amines induce selective release of lysosomal enzymes from mouse macrophages. Biochem. J. **188**, 933–936

35  Imort, M., Zühlsdorf, M., Feige, U., Hasilik, A. and von Figura, K. (1983) Biosynthesis and transport of lysosomal enzymes in human monocytes and macrophages. Effects of ammonium chloride, zymosan and tunicamycin. Biochem. J. **214**, 671–678

36  Keizer, H. G. and Joenje, H. (1989) Increased cytosolic pH in multidrug-resistant human lung tumor cells: effects of verapamil. J. Natl. Cancer Inst. **81**, 706–709

37  Willingham, M. C., Cornwell, M. M., Cardarelli, C. O., Gottesman, M. M. and Pastan, I. (1986) Single cell analysis of daunomycin uptake and efflux in multidrug-resistant and -sensitive KB cells: effects of verapamil and other drugs. Cancer Res. **46**, 5941–5946

38  Kornfeld, S. (1986) Trafficking of lysosomal enzymes in normal and disease states. J. Clin. Invest. **77**, 1–6

39  von Figura, K. and Hasilik, A. (1986) Lysosomal enzymes and their receptors. Annu. Rev. Biochem. **55**, 167–193

40  Tanaka, Y., Harada, R., Himeno, M. and Kato, K. (1990) Biosynthesis, processing, and intracellular transport of lysosomal acid phosphatase in rat hepatocytes. J. Biochem. (Tokyo) **108**, 278–286

41  Demaurex, N. (2002) pH homeostasis of cellular organelles. News Physiol. Sci. **17**, 1–5

42  Ma, L. and Center, M. S. (1992) The gene encoding vacuolar H⁺-ATPase subunit C is overexpressed in multidrug-resistant HL60 cells. Biochem. Biophys. Res. Commun. **182**, 675–681